Available online at www.sciencedirect.com
ScienceDirect
Geochimica et Cosmochimica Acta 73 (2009) 4998–5017
Geochimica et Cosmochimica Acta
www.elsevier.com/locate/gca

Timescales for the evolution of oxygen isotope compositions in the solar nebula

J.R. Lyons [a,*], E.A. Bergin [b], F.J. Ciesla [c,1], A.M. Davis [d], S.J. Desch [e], K. Hashizume [f], J.-E. Lee [g]

[a] *Intitute of Geophysics and Planetary Physics, University of California, Los Angeles, CA 90095, USA*
[b] *Department of Astronomy, University of Michigan, Ann Arbor, MI 48109, USA*
[c] *Department of Terrestrial Magnetism, Carnegie Institution of Washington, Washington, DC 20015, USA*
[d] *Department of Geophysical Sciences and Enrico Fermi Institute, University of Chicago, Chicago, IL 60637, USA*
[e] *School of Earth and Space Exploration, Arizona State University, Tempe, AZ 85287-1404, USA*
[f] *Department of Earth and Space Sciences, Osaka University, Osaka 560-0043, Japan*
[g] *Department of Astronomy and Space Science, Astrophysical Research Center for the Structure and Evolution of the Cosmos, Sejong University, Seoul 143-747, Republic of Korea*

Received 28 April 2008; accepted in revised form 22 January 2009; available online 21 May 2009

Abstract

We review two models for the origin of the calcium-, aluminum-rich inclusion (CAI) oxygen isotope mixing line in the solar nebula: (1) CO self-shielding, and (2) chemical mass-independent fractionation (MIF). We consider the timescales associated with formation of an isotopically anomalous water reservoir derived from CO self-shielding, and also the vertical and radial transport timescales of gas and solids in the nebula. The timescales for chemical MIF are very rapid. CO self-shielding models predict that the Sun has $\Delta^{17}O_{SMOW} \sim -20‰$ (Clayton, 2002), and chemical mass-independent fractionation models predict $\Delta^{17}O_{SMOW} \sim 0‰$. Preliminary Genesis results have been reported by McKeegan et al. (McKeegan K. D., Coath C. D., Heber, V., Jarzebinski G., Kallio A. P., Kunihiro T., Mao P. H. and Burnett D. S. (2008b) The oxygen isotopic composition of captured solar wind: first results from the Genesis. *EOS Trans.* AGU 89(53), *Fall Meet*. Suppl., P42A-07 (abstr)) and yield a $\Delta^{17}O_{SMOW}$ of $\sim -25‰$, consistent with a CO self-shielding scenario. Assuming that subsequent Genesis analyses support the preliminary results, it then remains to determine the relative contributions of CO self-shielding from the X-point, the surface of the solar nebula and the parent molecular cloud.

The relative formation ages of chondritic components can be related to several timescales in the self-shielding theories. Most importantly the age difference of ~1–3 My between CAIs and chondrules is consistent with radial transport from the outer solar nebula (>10 AU) to the meteorite-forming region, which supports both the nebular surface and parent cloud self-shielding scenarios. An elevated radiation field intensity is predicted by the surface shielding model, and yields substantial CO photolysis (~50%) on timescales of 0.1–1 My. An elevated radiation field is also consistent with the parent cloud model. The elevated radiation intensities may indicate solar nebula birth in a medium to large cluster, and may be consistent with the injection of ^{60}Fe from a nearby supernova and with the photoevaporative truncation of the solar nebula at KBO orbital distances (~47 AU). CO self-shielding is operative at the X-point even when H_2 absorption is included, but it is not yet clear whether the self-shielding signature can be imparted to silicates. A simple analysis of diffusion times shows that oxygen isotope exchange between ^{16}O-depleted nebular H_2O and chondrules during chondrule formation events is rapid (~minutes), but is also expected to be rapid for most components of CAIs, with the exception of spinel. This is consistent with the observation that spinel grains are often the most ^{16}O-rich component of CAIs, but is only broadly consistent with the greater degree of

* Corresponding author.
E-mail address: jimlyons@ucla.edu (J.R. Lyons).
[1] Present address: Department of the Geophysical Sciences, University of Chicago, Chicago, IL 60637, USA.

doi:10.1016/j.gca.2009.01.041

exchange in other CAI components. Preliminary disk model calculations of self-shielding by N_2 demonstrate that large $\delta^{15}N$ enrichments ($\sim +800‰$) are possible in HCN formed by reaction of N atoms with organic radicals (e.g., CH_2), which may account for ^{15}N-rich hotspots observed in lithic clasts in some carbonaceous chondrites and which lends support to the CO self-shielding model for oxygen isotopes.

1. INTRODUCTION

The implications of the CAI oxygen isotope mixing line (Clayton et al., 1973) for meteorite and solar system formation have been debated for over three decades. Clayton and Mayeda (1984) recognized that the CAI line was the result of mixing between a ^{16}O-rich silicate reservoir and ^{16}O-poor water reservoir, but the origin of the water reservoir was unknown. Clayton (2002) proposed that self-shielding during CO photodissociation produces an abundance-dependent fractionation in the rare isotopologues of CO, a process well known in molecular clouds (Bally and Langer, 1982) and previously discussed for the solar nebula (Thiemens and Heidenreich, 1983; Navon and Wasserburg, 1985). The resulting O atoms, highly enriched in ^{17}O and ^{18}O compared to the initial composition, combine with H_2 by various reactions to form the hypothesized isotopically heavy H_2O reservoir. The H_2O reacts rapidly with silicates and silicate precursors (e.g., SiO) to enrich inner solar system materials in ^{17}O and ^{18}O, with the exception of CAIs. If CAIs and ^{16}O-rich forsterite are condensates from a solar gas (Grossman, 1972), they are representative of the bulk molecular cloud from which the Sun and the solar nebula formed (e.g., Krot et al., 2002). With respect to oxygen isotopic composition, the most ^{16}O-rich CAIs should be similar to the Sun, assuming that gas–dust isotopic mass fractionation has not occurred in the solar nebula prior to or during the time of CAI formation. Therefore, a necessary test of the self-shielding scenario is measurement of the oxygen isotope composition of the Sun, which should be similar to the most ^{16}O-rich CAIs.

The main competing hypothesis for the formation of the CAI mixing line is chemical mass-independent fractionation of oxygen isotopes during high-temperature reaction of silicate oxide precursors (Marcus, 2004). This idea evolved from the discovery of chemical MIF during the gas-phase formation of ozone (Thiemens and Heidenreich, 1983). The origin of the chemical MIF is believed to be the non-equilibrium distribution of energy states in the vibrationally excited O_3, which are dependent on the symmetry of the ozone isotopomers (Gao and Marcus, 2001). Marcus (2004) employed similar arguments for XO_2 formation, where X = a rock forming element (e.g., Si, Al, Ti). In terms of the CAI mixing line, chemical MIF forms the CAIs with a negative $\Delta^{17}O$ value from initial material with a bulk oxygen isotope composition that is approximately terrestrial. Thus, the Sun is predicted to have a $\Delta^{17}O$ value that is also approximately terrestrial.

Given the variety of processes and locations that have been proposed for creating the ^{16}O-depleted end member reservoir of the CAI mixing line, there are a large number of relevant timescales to be considered. Our focus here will be primarily on the physical and chemical timescales associated with CO self-shielding, with a short discussion of mass-independent fractionation (MIF) in high-temperature CAI-forming reactions. The preliminary results for the oxygen isotopic composition of the solar wind from Genesis (McKeegan et al., 2008b) are not in agreement with supernova injection of oxygen into the disk after formation of the Sun (Gounelle and Meibom, 2007). We will not address the suggestion that galactic chemical evolution is responsible for the ^{16}O enrichment of CAIs (Clayton, 1988).

The recent discovery of magnetite and pentlandite grains in Acfer 094 matrix highly enriched in ^{17}O and ^{18}O along a long extension of slope-1 CAI mixing line (Sakamoto et al., 2007; Seto et al., 2008) lends credence to the idea that CO self-shielding formed an ^{16}O-depleted H_2O reservoir, with subsequent exchange of oxygen during low temperature oxidation (and sulfidization) of the metal grains. This scenario is consistent with recent model predictions for self-shielding at low temperatures (Yurimoto and Kuramoto, 2004; Lyons and Young, 2005a; Lee et al., 2008). To be consistent with the X-wind self-shielding scenario, ^{16}O-rich water would have to be transported to lower temperature locations. The case made for self-shielding at any location is not proven until both the size of the ^{16}O-depleted reservoir and the oxygen isotopic composition of the Sun are known. The implications for the chemical mass-independent mechanism (Thiemens, 1988, 1999, 2006; Marcus, 2004) remain to be investigated.

A schematic view of the solar nebula is shown in Fig. 1. Region 1 is the hot, thermally ionized, low-dust, inner solar nebula, and is MRI (magnetorotational instability) active. Region 2 is the MRI-dead zone (Gammie, 1996), and is separated from region 1 by the dust front. Region 3 is the MRI-active nebular surface. Region 4 is the outer nebula which is generally MRI-active if the dust content is sufficiently low. Region 5 represents disk accretion during collapse of the parent molecular cloud. Material accreting to the disk passes through a weak shock with shock temperatures – several hundred Kelvin, enough to vaporize ices but not silicates (Lyons and Young, 2005b). CO self-shielding has been proposed to occur in regions 1 (Clayton, 2002) and 3 (Lyons and Young, 2005a), and in the parent molecular cloud (Yurimoto and Kuramoto, 2004; Lee et al., 2008) which then accretes onto the disk at region 5. MRI-induced vertical mixing is expected in region 4. Chemical mass-independent fractionation reactions have been proposed to occur in region 1 (Marcus, 2004). The dead zone (region 2) has not yet been quantitatively included in oxygen isotope radial transport models. The outer boundary of the dead zone is unknown but is expected to be tens of AU (e.g., Sano et al., 2000). Observations and modeling of disk spectral energy distributions (SEDs) are interpreted as providing evidence for an inflated inner rim in region 1 (Dullemond et al., 2001), which is not shown in Fig. 1.

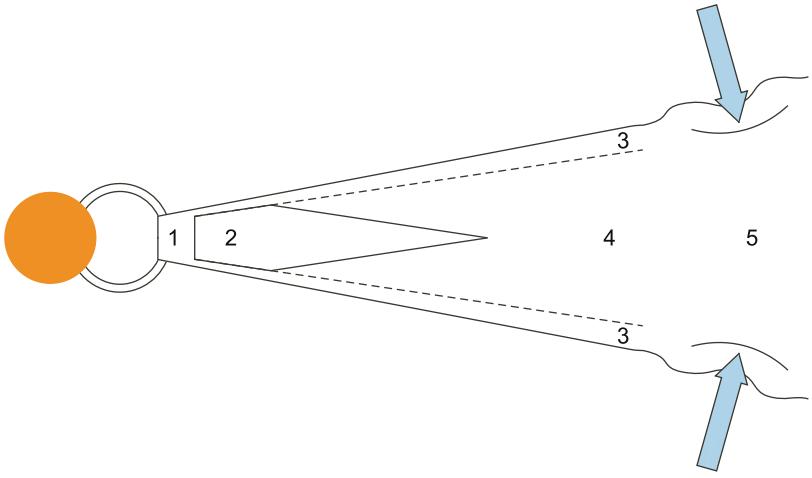

Fig. 1. Schematic of dynamical regions of the solar nebula. Region 1 is thermally ionized and MRI-active and has flux tubes extending from the inner disk to the protosun. Region 2 is the 'dead zone' (MRI inactive). Region 3 is the disk surface which is partially ionized and MRI-active. Region 4 is ionized by cosmic rays and is MRI-active. Region 5 undergoes active accretion (blue arrows) from the collapsing parent cloud. Shock fronts are indicated by curved solid line. (Figure after Gammie, 1996).(For interpretation of color mentioned in this figure the reader is referred to the web version of the article.)

An inflated region will shadow a portion of the disk surface from direct protostellar radiation out to a distance of ~10 AU.

The ages of formation of the components of chondritic meteorites are essential to understanding the evolution of the solar nebula inside the snow line. The principal chondrite components are chondrules, CAIs, amoeboid olivine aggregates (AOAs), metal, and matrix material. CAIs formed by condensation from a ^{16}O-rich gas ($\Delta^{17}O = \delta^{17}O - 0.52\delta^{18}O \sim -20‰$ to $-25‰$) of approximately solar composition (Yoneda and Grossman, 1995), although most have been remelted early in solar system history (Grossman et al., 2000). Most chondrules and matrix material formed in a ^{16}O-depleted gas ($\Delta^{17}O > -10‰$) under more oxidizing conditions and at lower temperatures (<1000 K). Chondrules formed ~1–3 My later than CAIs for the CV, CR and CB chondrites (Amelin et al., 2002; see also review by Krot et al., 2009). Most CAIs have been remelted early in solar system history, well before chondrule formation, but a small fraction were remelted later during chondrule formation conditions. The ^{26}Al–^{26}Mg chronometer has constrained the duration of formation of CV CAIs to be <20–30 Ky (Jacobsen et al., 2008). The correlation between age and oxygen isotope composition of CAIs/AOAs and chondrules/matrix suggests that oxygen isotope evolution occurred in the planet-forming region of the solar nebula on a timescale ~1 My (e.g., Krot et al., 2005). Here, we address the timescales of oxygen isotope evolution inherent in CO self-shielding and chemical mass-independent fractionation models of the solar nebula.

2. RECENT MEASUREMENTS

The key unknown in understanding oxygen isotopes in the solar system is the oxygen isotopic composition of the Sun. There are several models that seek to explain the distribution of oxygen isotopic composition in the solar system through UV self-shielding (Clayton, 2002; Yurimoto and Kuramoto, 2004; Lyons and Young, 2005a; Lee et al., 2008) or chemical reactions that cause mass-independent fractionation (Thiemens, 1988, 1999, 2006; Marcus, 2004). The self-shielding models disagree on where self-shielding might have occurred, but agree that the Sun should have about the same isotopic composition as the most ^{16}O-rich minerals in CAIs, $\delta^{17}O \sim \delta^{18}O \sim -50‰$. The chemical models suggest that the Sun should have about the same oxygen isotopic composition as the Earth. Spectroscopic measurements of the solar photosphere give an ^{18}O/^{16}O ratio corresponding to $\delta^{18}O = 41^{+63}_{-61}‰$ (see review by Davis et al., 2008; 1σ errors), which is permissive of all models, and no spectroscopic data are available for ^{17}O.

We summarize here the recent progress towards the identification of the oxygen isotopic composition of the solar wind implanted in lunar regolith samples. The surface of the Moon has been exposed over billions of years to irradiation by solar ions and to contributions of various extraterrestrial sources, including interplanetary dust particles, micrometeorites, meteorites and comets. From studies of nitrogen isotopes among various lunar soils sampled at different locations, a competition of at least two fluxes with different origins (solar wind and micrometeorites) accreting onto the Moon surface was clearly observed (Hashizume et al., 2002).

Two groups have attempted to measure solar wind oxygen implanted in lunar metal grains, and have reached opposite conclusions. Hashizume and Chaussidon (2005) reported the presence among metallic grains from lunar sample 79035 of a deeply implanted oxygen component enriched in ^{16}O ($\Delta^{17}O < -20 \pm 4‰$). Silicate grains from this sample were enriched in D-depleted hydrogen ($\delta D < -930‰$; Hashizume et al., 2000) and solar noble gases (Wieler et al., 1999; Hashizume et al., 2002), suggesting not only enrichment of the solar component in this

sample, but a relatively low contribution of components that carry D-rich hydrogen, like the asteroidal components. From this sample, they estimated the protosolar isotopic compositions of nitrogen (Hashizume et al., 2000) and carbon (Hashizume et al., 2004) and they inferred that the observed ^{16}O-enriched component had a solar origin. However, Ireland et al. (2006) came to a contrasting conclusion from the finding of a ^{16}O-depleted component ($\Delta^{17}O = +26 \pm 3‰$) at the surface of metallic grains from a solar noble-gas-rich lunar regolith 10084, which they likewise argued to have a solar origin.

The two groups have continued their analyses of lunar samples during the last several years. Ireland et al. (2007) reported the results of the oxygen isotope analyses among metallic grains from two regolith samples (61141 and 78481) which are considered to be exposed fairly recently at the lunar surface. They did not find other components beside the isotopically normal ($\Delta^{17}O = 0‰$) component in these grains. Hashizume and Chaussidon (2008) analyzed the small metallic grains from the 79035 sample which was left unmeasured in their previous analyses (Hashizume and Chaussidon, 2005), and several grains from sample 71501, a recently exposed solar noble-gas-rich sample. In contrast to the case of Ireland et al. (2007), widely different $\Delta^{17}O$ values were detected among the grains ($-11 \pm 4 < \Delta^{17}O < +33 \pm 3‰$), confirming all earlier results. However the negative $\Delta^{17}O$ values were not as extreme as those observed by Hashizume and Chaussidon (2005) ($<-20‰$), likely due to the increased contribution of the normal components ($\Delta^{17}O = 0$ ‰) commonly observed among the lunar grains. The ^{16}O-enriched component was found among grains from both the 79035 and 71501 samples. Hashizume and Chaussidon (2008) further inferred that the ^{16}O-depleted (positive $\Delta^{17}O$) component probably did not come from the Sun. This is because of the more than one order of magnitude higher concentration of the ^{16}O-depleted component in the 79035 grains, compared to the estimated range of the solar oxygen concentrations based on the solar noble gas measured among many grains from this sample (Wieler et al., 1999; Hashizume et al., 2002). The concentration of the ^{16}O-enriched component is within this expected solar concentration range, leading them to argue that the solar component is ^{16}O-rich. Their results suggest the supply to the Moon of two extraselenial components with different origins. Further work is required to precisely resolve the different information recorded grain-by-grain among the lunar samples.

The Genesis mission collected solar wind and returned collectors to Earth. The most anticipated result is the oxygen isotopic composition of the solar wind. McKeegan et al. (2008a) report that there is sufficient oxygen in the SiC target from the Genesis solar wind concentrator to measure and that contamination can be controlled. Preliminary Genesis results have just been reported (McKeegan et al., 2008b) and show that the solar wind has a $\Delta^{17}O$ of about $-25 \pm 15‰$ (2σ errors, counting statistics only) based on seven analyses. An eighth analysis at a location on the SiC target displaced from the other seven by about 9 mm has $\Delta^{17}O = -8 \pm 20‰$, and is consistent with either the terrestrial fractionation line or a mass-dependent line intersecting the other seven analyses. Mass-dependent fractionation across the target is expected due to the electrostatic concentrator (Wiens et al., 2003). Matrix effects due to differences in the composition of the Genesis SiC targets from that of the magnetite standard may introduce additional mass-dependent inaccuracies in the calculated solar wind isotopic composition. The preliminary results appear to rule out a Sun depleted in ^{16}O, and even an isotopically terrestrial Sun. The Sun is apparently ^{16}O-rich; although it is not known at the present time whether the composition lies along the CAI mixing line because of uncertainties in mass-dependent corrections to the data, we will assume hereafter that it does lie on this line. The self-shielding models are consistent with the Genesis results, but the chemical mass-independent fractionation models (e.g., Marcus, 2004) are not, at least in their current form.

It is useful to compare Genesis results with the lunar metal grain analyses of Hashizume and Chaussidon (2005). The solar wind ions collected by Genesis were implanted at a depth ~100 nm, as expected for multiply charged oxygen ions accelerated to a few tens of keV by the electrostatic concentrator (Ziegler et al., 1985; McKeegan et al., 2008a). The deeply implanted (100 nm to $\geqslant$ 1 μm) oxygen reported by Hashizume and Chaussidon (2005) was not observed in the preliminary Genesis analyses. The energy of solar energetic particles is too high to be reflected by the ion mirror in the concentrator and the fluence is far too low to be observed in nonconcentrator Genesis targets. Several technical issues concerning the measurements of the lunar grains, such as the range of depths of the analysis pits created in different ion microprobe measurements and the imprecise determination of the implantation depth, will be discussed by Hashizume and Chaussidon in a future publication.

Recently, very large oxygen isotope fractionation as a result of CO photodissociation has been demonstrated in the laboratory as an experimental test of self-shielding (Chakraborty et al., 2008). The photodissociation experiments were performed at wavelengths ~100 nm using a synchrotron source with a bandwidth of ~1 nm. CO_2 was formed from the O liberated from CO dissociation, and was isolated with cold traps. Isotopic analyses of the CO_2 show very large fractionations (>>2000‰) relative to the initial CO, and $\delta^{17}O/\delta^{18}O$ ratios that depend on wavelength (Chakraborty et al., 2008). Because the $\delta^{17}O/\delta^{18}O$ ratios differ from unity (e.g., 1.38 at 105.17 nm) and because the enrichments are so large, Chakraborty et al. argue that the large fractionations are not due to self-shielding but rather are a result of the photophysics of CO dissociation. The very large CO cross sections ($\sim 10^{-15}$ cm^2 at 105.17 nm) and the high column densities used in the experiments ($\sim 10^{18}$ cm^{-2}) imply that C^{16}O is, in fact, strongly self-shielding. Modeling CO self-shielding in the solar nebula using shielding functions (Lyons and Young, 2005a) yields large delta values for the molecules produced as a results of CO photodissociation, with $\delta^{17}O/\delta^{18}O$ ratios ~1.3 at early times (Section 5, Fig. 3), so even shielding functions can yield non-unity slopes. The experiments of Chakraborty et al. (2008) demonstrate the need for accurate spectra for CO isotopologues (e.g., Eidelsberg et al., 2006).

With such spectra a full integration over wavelength can be performed to evaluate isotopologue photodissociation rates, and the corresponding isotope delta values. The sum over all CO bands, and including absorption by H_2, will then tell us whether a slope near unity is expected for CO photodissociation in the solar nebula or parent cloud.

3. THE BIRTH ENVIRONMENT OF THE SUN

If the Sun formed in proximity to massive stars, a ready-made source of external UV radiation would be present, capable of photodissociating CO and leading to large isotopic fractionations. This would also be a very likely mode of star formation for the Sun to have taken, as the majority of Sun-like stars form in large clusters, as we argue below. Statistics alone do not require that the Sun formed in such an environment, but other evidence (e.g., the presence of live ^{60}Fe and the orbits of Kuiper belt objects) may, and can even provide broad constraints on the UV flux in the Sun's star-forming environment.

Most low-mass stars form in clusters containing at least hundreds of stars. A complete census of the nearest 2 kpc shows that 70–90% of all low-mass stars form in such environments (Lada and Lada, 2003). As the very largest star-forming clusters in Galaxy lie beyond 2 kpc, even this fraction may overestimate the fraction of Sun-like stars that form outside of clusters. Low-mass star formation in high-mass star-forming regions was reviewed by Hester and Desch (2005), to which the reader is referred for more details. Here we emphasize that formation in rich clusters (>100 stars) is common.

Of those stars born in rich clusters, defined as containing 10^2–10^6 stars, it is essentially the case that as many stars form in clusters with $\sim 10^2$ stars as in clusters with $\sim 10^6$ stars. This is a consequence of the fact that the cluster initial mass function scales as $dN/dM \sim M^{-2}$ (Elmegreen and Efremov, 1997), where N is the number of clusters of mass M. The number of stars formed in clusters with mass $M_1 < M < M_2$ is $\frac{1}{<M_*>}\int_{M_1}^{M_2}\frac{dN}{dM}MdM \propto \log\left(\frac{M_2}{M_1}\right)$ where $<M^*>$ is the mean stellar mass, so that roughly equal numbers of stars are produced per decade in mass. Massive stars in the cluster provide the bulk of the ionizing UV radiation, and consideration of the orbit of a protostellar system in the cluster relative to the massive star or stars (assumed to be at the cluster center) allows a mean UV flux to be estimated due to the cluster radiation. Within a cluster with N stars, the average UV flux experienced by a solar system is $F_{UV} = 1.6 \times 10^{12}\ (N/2000)\ d^{-2}$ photons cm^{-2} s^{-1} (Adams and Laughlin, 2001), where d is the spatial scale of the cluster in parsecs. For comparison, the ionizing UV radiation due to the central star is $F_{UV} = 3.5 \times 10^{13}\ R^{-2}$ photons cm^{-2} s^{-1}, where R is the distance to the central star in AU, which is smaller than the cluster radiation beyond $R = 5$ AU for a cluster with $N = 2000$ and $d = 1$ pc (Adams and Laughlin, 2001). Assuming an average photon energy of 20 eV and scaling to the Habing flux ($G_0 = 1$ for a UV flux of 1.6×10^{-3} erg cm^{-2} s^{-1}), we find $G_0 \approx 3 \times 10^4\ (N/2000)\ d^{-2}$. Very roughly, then, perhaps a third of all Sun-like stars form outside rich clusters with external $G_0 \approx 1$ (and for which the UV flux from the protostar dominates), an equal number form in small clusters ($N = 10^2$–10^4, $d = 1$–2 pc) for which $G_0 \approx 1 \times 10^3$–$3 \times 10^4$, and another third form in even larger clusters ($N = 10^4$–10^6, $d \approx$ several pc) for which $G_0 \approx 3 \times 10^4$–$1 \times 10^5$. Examples of these different star formation regions would be, respectively, the Taurus Molecular Cloud, the Orion Nebula Cluster and the Carina Nebula. These simple arguments suggest $G_0 = 10^3$–10^5 is common during star formation. A more sophisticated analysis by Fatuzzo and Adams (2008) including integration over cluster sizes and orbital motions of stars in the cluster environment, and other factors, confirms that $G_0 \approx 10^3$–10^4 is the most probable degree of irradiation for the solar system to have experienced.

The above arguments show that high UV fluxes are a typical feature of low-mass star formation, but several lines of evidence directly put the formation of the solar system in a cluster environment, and even suggest a likely range of G_0. The early solar system contains radionuclides such as ^{60}Fe that are most plausibly explained by injection into the solar nebula by a nearby supernova (see review by Wadhwa et al., 2007). For a cluster to be likely to contain a star massive enough to go supernova, it must contain at least about 2000 stars (Adams and Laughlin, 2001), implying $G_0 \sim 10^4$. It is possible that ^{60}Fe was inherited from the interstellar medium (ISM) rather than directly injected into the disk from a nearby supernova. Gounelle and Meibom (2008) argue for this origin of ^{60}Fe, and offer specific criticisms against an intracluster supernova origin of ^{60}Fe, based on the timing and location of the protosolar disk within a cluster (e.g., massive star lifetimes are ~3–5 My, too long to have injected ^{60}Fe into the protosolar disk within ~1 My of its formation). High initial values of ^{60}Fe/^{56}Fe ($>10^{-6}$) in the solar nebula would only be explained by local supernova injection. Slightly lower meteoritic values are currently favored (3×10^{-7}, Wadhwa et al., 2007). Low values of ^{60}Fe/^{56}Fe may be explained by supernova injection or by inheritance from the ISM. At this time, it is not clear how much ^{60}Fe can be inherited from the ISM (Wasserburg et al., 1996; Hester and Desch, 2005), and so the question of the origin of ^{60}Fe is still open. ^{60}Fe is suggestive of a cluster origin for the Sun, but the issue is not closed.

More direct arguments come from the structure of the solar system. The Kuiper Belt exhibits a prominent dearth of objects with semimajor axes beyond 47 AU (Trujillo and Brown, 2001). Proposed explanations for this sharp "edge" of the Kuiper Belt include stellar encounters that dynamically truncate the disk (Laughlin and Adams, 1998; Ida et al., 2000), or external photoevaporation (Adams et al., 2004). The distant perihelia of Kuiper Belt Objects (KBOs) like Sedna in fact require a stellar encounter at some point, a scenario only likely if the Sun formed in a rich cluster environment (Kenyon and Bromley, 2004). An outer edge due to photoevaporation is consistent with $G_0 \approx 3 \times 10^3$–$3 \times 10^4$ on timescales of 2–5 My (shorter timescale for higher G_0) at 47 AU (Adams et al., 2004). Recently Desch (2007) examined the initial surface density of the solar nebula and found it was characterized by a very steep profile that is consistent with a steady-state decretion disk (a disk that is losing mass) that is being photoevapo-

rated, providing corroboration for the photoevaporation model and with similar values for G_0. Another possible cause of the lack of KBOs beyond 47 AU is the depletion of outer solar system solids due to gas drag migration (Ciesla and Cuzzi, 2006, and references therein).

In summary, it is most probable that solar systems like ours formed in rich clusters with $G_0 \approx 10^3$–10^4, and independent lines of evidence (short-lived radionuclides, the dynamical properties of planets and Kuiper Belt objects, and the mass distribution of the solar nebula) confirm that our solar system did indeed form in such an environment. The intersection of G_0 constraints from these three lines of evidence favors $G_0 \approx 3 \times 10^3$–$1 \times 10^4$. However, many uncertainties are present in the above arguments, and we propose that the range in G_0 considered in self-shielding models should be $G_0 \sim 1 \times 10^3$–3×10^4.

4. THE INNER SOLAR NEBULA

The hot, dense inner nebula (region 1 of Fig. 1) is the location for CO self-shielding suggested by Clayton (2002), and the most likely place for proposed MIF-producing CAI/silicate reactions (Marcus, 2004). The chemical timescales here are rapid ($<<10^4$ y) due to the high-temperatures, high gas density and large photon flux.

4.1. High-temperature CO self-shielding

For CO self-shielding, O liberated during CO photolysis reacts immediately with H_2 to form H_2O at temperatures >1000 K. H_2O then passes the MIF signature to silicate precursors. However, at higher temperatures the magnitude of the MIF signature produced during self-shielding is reduced by H_2 absorption. Fig. 2 illustrates this for the CO $E^1\Pi(1)$–$X^1\Sigma^+(0)$ band in which H_2 absorption has been included in the line-by-line calculation. The figure shows the δ-values for total H_2O (disk $H_2O + H_2O$ derived from CO photolysis) at the disk midplane at gas temperatures of 50, 300 and 1500 K, corresponding to distances of 30, 0.87, and 0.035 AU, respectively. At 1500 K the MIF signature of H_2O is high enough to raise silicates from ~−50‰ to ~0‰, but only in $\delta^{17}O$. At 300 K and 50 K very large MIF signatures are predicted for this band of CO. The calculations for Fig. 2 only include the photolysis of CO isotopologues, so that reactions to reform CO are not accounted for. It is for this reason that the MIF signature at 50 K is much larger than obtained in Lyons and Young (2005a). The reduction in the amplitude of the MIF signature decreases with increasing temperature due to absorption by H_2 and a reduction in the CO cross sections. The steep slope at 1500 K is the result of coincident structure in the computed H_2 and $C^{18}O$ spectra (Lyons et al., 2008).

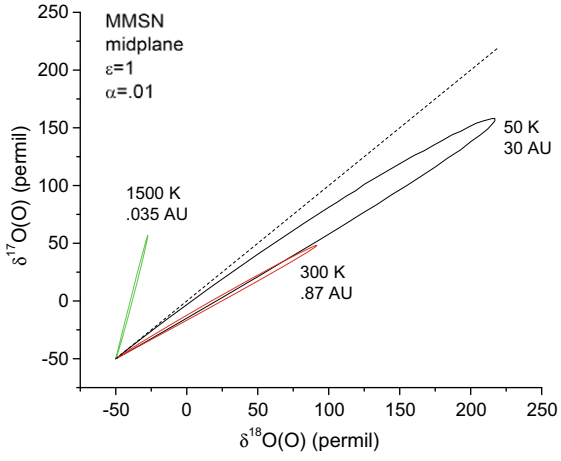

Fig. 2. CO self-shielding in the $E^1\Pi(1)$-$X^1\Sigma^+(0)$ band at various temperatures and disk locations, including the effects of H_2 absorption (Lyons et al., 2008). The model assumes a modern solar flux that scales as $1/R^2$ but with no enhancement ($\varepsilon = 1$), and a turbulent viscosity parameter $\alpha = 10^{-2}$. Only CO photolysis has been considered; reactions forming H_2O and reforming CO have been neglected. The results shown are for the disk midplane ($Z = 0$) with peak δ-values occurring at 90, 60 and 50 ky at 30, 0.87 and .035 AU, respectively.

The 3-isotope trajectories in Fig. 2 are for a single band of CO. That one band out of about 20 active bands (some bands are completely shielded by H_2 absorption) can yield trajectories far from the slope-1 line defined by CAIs is not surprising. However, if self-shielding is in fact the mechanism responsible for the CAI mixing line, the sum over all active CO bands must yield a slope-1 trajectory for nebular H_2O. The wavelength dependence of the experimental results of Chakraborty et al. (2008) for photolysis of CO by synchrotron FUV radiation also demonstrates the need to sum over all bands. Similarly, although probably of secondary importance, if self-shielding occurs at multiple disk/cloud locations at different temperatures, the sum over all locations must yield a slope of close to unity.

4.2. Chemical mass-independent fractionation

The chemical mass-independent fractionation model (Marcus, 2004) assumes $\Delta^{17}O = \delta^{17}O$–$0.52\ \delta^{18}O \sim 0‰$ (relative to SMOW) in the Sun and bulk solar nebula. This is in contrast to the CO self-shielding models (Clayton, 2002; Yurimoto and Kuramoto, 2004; Lyons and Young, 2005a) which require that silicates initially have $\Delta^{17}O = \sim -25‰$ (i.e., like the majority of ^{16}O-rich CAIs), and are later altered or modified by a ^{16}O-poor water vapor. As already noted, the preliminary Genesis results indicate $\Delta^{17}O \sim -25‰$ for the solar wind (McKeegan et al., 2008b), and so favor the CO self-shielding models. However, because these are preliminary results, and because chemical MIF reactions may still occur in the solar nebula, we consider the MIF models in more detail.

The archetypal example of chemical mass-independent fractionation is the gas-phase formation of ozone (Thiemens and Heidenreich, 1983). The formation mechanism for the asymmetric isotopomer is shown in reaction scheme I,

$$\begin{array}{c} O + QO \underset{k_{-a}}{\overset{k_a}{\rightleftharpoons}} QOO^* \xrightarrow{k_b} OQ + O \\ \downarrow M \\ QOO \end{array} \qquad \text{(I)}$$

where QOO^* is the vibrationally excited intermediate, Q is either ^{17}O or ^{18}O, and M is a background molecule that provides collisional stabilization to QOO. The source of the mass-independent anomaly is proposed to be a slight deficiency in the redistribution of intramolecular energy (i.e., the vibrational quanta) of the symmetric isotopomer, OQO^*, relative to QOO^* (Gao and Marcus, 2001, 2002). This is expressed as a lower density of states for OQO^* versus QOO^*, so that k_b and k_{-a} are larger for OQO^* than for QOO^*, yielding an excess of QOO formation relative to OQO. The excess in QOO occurs for both $Q = {}^{17}O$ and ^{18}O, and therefore produces a chemical MIF signature. The deficiency in intramolecular energy redistribution occurs for the symmetric isotopomers because there are roughly half as many states available as for the asymmetric isotopomers, making anharmonic and other couplings less effective (Gao and Marcus, 2001; Marcus, 2008). Application of unimolecular dissociation theory, with the inclusion of the symmetric density of states at a value ~85% of the statistical density of states, yields excellent agreement (Gao and Marcus, 2001, 2002) with measured isotopomer-specific rate coefficients (Mauersberger et al., 1999), and with the measured temperature and pressure dependence of the MIF signature in ozone (Gao and Marcus, 2007).

It has been proposed (e.g., Thiemens, 1999) that symmetry-dependent isotopic reactions analogous to O_3 formation occurred among CAI precursors in hot regions of the solar nebula. Specifically, gas phase reactions such as $O + SiO \overset{M}{\leftrightarrows} SiO_2^* \rightarrow SiO_2$ could yield mass-independent products. Marcus (2004) showed that such 3-body gas phase reactions are far too slow to compete with reaction of O with H_2. At 2000 K and 1 mbar, and assuming $H_2/CO \sim 10^3$, the rate of reaction of O with H_2 exceeds the rate of O addition to SiO by a factor of $\sim 10^9$. The likelihood of gas-phase formation of compounds such as SiO_2 would be greater at higher pressures (>> 1 mbar), in the presence of significant dust enhancements, and if H_2 has been removed preferentially relative to CO.

As an alternative to gas phase reactions producing MIF in the solar nebula, it has been shown (Marcus, 2004, 2008; Young et al., 2008) that reactions on surfaces greatly increase the probability of reaction. The mechanism for silicates is proposed to operate at high-temperatures and on the surface of a growing CAI grain. Surface reactions between O and XO, where X = Si, Ca, Al, etc., provide an entropic rate enhancement of $\sim 10^6$ over gas phase reactions. (In transition state theory, the rate coefficient of reaction is $k_{TST} = (kT/h)e^{-\Delta G^{\neq}}$, where $\Delta G^{\neq} = \Delta H^{\neq} - T\,\Delta S^{\neq}$ is the Gibbs free energy of activation and $\Delta H^{\neq}$ and $\Delta S^{\neq}$ are the enthalpy and entropy of activation, respectively. Rate enhancement can arise from a decrease in $\Delta H^{\neq}$ and/or an increase in $\Delta S^{\neq}$. The latter contributes most to rate enhancement in surface reactions.) The surface MIF mechanism is postulated to be symmetry-dependent, with OXO as the symmetric species, and OXQ as the asymmetric species. The mechanism for OXQ(ads) formation, where OXQ(ads) is the adsorbed species, is shown in reaction scheme II. The reaction scheme includes CAI growth by uptake of adsorbed species, evaporation of adsorbed species, and uptake of gas phase oxygen, O_{1-w}, as dictated by the stoichiometry of the various CAI minerals. w is the fraction of O in SiO_2 units to total O in a given CAI mineral, and represents the fraction of adsorbed O that is incorporated into the CAI; $w \sim ½$ for most CAIs (Marcus, 2004). The source of O(ads) in scheme (II) is either binding of O atoms directly from the hot nebular gas onto the CAI grain surface, or a surface disproportionation of nebular H_2O on the grain to produce O(ads) and H_2. Because of the much greater concentration of H_2O in the nebula, Marcus (2004) favors the H_2O disproportionation reaction as the primary source of O(ads).

$$\begin{array}{ccccc} O(ads) + XQ(ads) & \underset{k_{-a}}{\overset{k_a}{\rightleftharpoons}} & OXQ^*(ads) & \xrightarrow{k_b} & Q(ads) + XO(ads) \\ \searrow \swarrow k_c & & \downarrow M & & \searrow \swarrow k_c \\ CAI & & OXQ(ads) & & CAI \\ \uparrow & & \downarrow evap & & \uparrow \\ O_{1-w} & & OXQ & & O_{1-w} \end{array} \qquad \text{(II)}$$

At the high-temperatures of CAI formation (~1500–2000 K), the mass-independent mechanism will yield similar isotope fractionations for ^{17}O and ^{18}O, so a single quantity, δQ, may be used to define both. To obtain $\delta Q \sim -50‰$ relative to the bulk solar nebula for CAIs (in the vicinity of CAI formation) requires a density of states of the symmetric adsorbed species to be ~0.90 of the statistical value, while the asymmetric adsorbed species has a fully statistical density of states. These values are very similar to those determined for ozone (Gao and Marcus, 2001). Laboratory experiments are needed to determine whether MIF effects do in fact occur during high-temperature surface reactions.

We consider here the internal consistency of the MIF scenarios by considering the implications of isotopic mass balance. Accretion onto the disk and accretion onto the protosun from the disk implies that the solar nebula is not a closed system. In addition, mass loss from the protosun-nebula system occurs via bipolar jets and high-velocity disk winds, and later (after several My) as a result of photoevaporation of nebular gas. In the discussion of chemical MIF presented below, we assume that the solar nebula in the region of CAI formation may be considered a closed system with respect to $\Delta^{17}O$. By contrast, in the CO self-shielding scenario loss of CO via photoevaporation in the later stages of nebular evolution may represent a significant flux of low-$\Delta^{17}O$ material from the nebula, which would yield planets with bulk $\Delta^{17}O$ different from the Sun.

A key test of the surface MIF mechanism (Marcus, 2004) is to determine if it can self consistently explain the

isotope anomalies in both CAIs and in nebular H_2O. Based on analyses of Murchison, Clayton and Mayeda (1984) inferred that initial nebular water (gas) had a minimum $\Delta^{17}O$ of 6.3–8.6‰. The observation of a mass-independent anomaly in magnetite grains in the Semarkona meteorite (Choi et al., 1998) argues for nebular water enriched in ^{17}O relative to SMOW. The magnetite grains are believed to have formed by the reaction $3Fe^0 + 4H_2O \rightarrow Fe_3O_4 + 4H_2$, and so $\Delta^{17}O$ of magnetite reflects nebular water. The mean $\Delta^{17}O$ measured by Choi et al. (1998) is $\sim +5.0‰$. Because of the possibility of isotope exchange with other phases during alteration, the Choi et al. (1998) results should be considered a minimum value for nebular water. The highly ^{16}O-depleted magnetite and pentlandite grains ($\Delta^{17}O \sim +70$–$85‰$ and $\delta^{17}O/\delta^{18}O \sim 1$) discovered in Acfer 094 (Sakamoto et al., 2007; Seto et al., 2008) are ~10 μm in size and have an abundance of ~100 ppm by mass. They were most likely formed during alteration reactions with nebular water, and so provide evidence for a (small) reservoir of nebular water highly enriched in ^{17}O and ^{18}O.

The chemical MIF mechanism predicts that both nebular water and non-CAI silicates have $\Delta^{17}O > 0$ (Marcus, 2004). According to reaction scheme II (with X = Si), SiO_2(ads) is formed on the CAI surface, and then evaporates adding SiO_2 with $\Delta^{17}O > 0$ to the nebular gas. Formation of H_2O with $\Delta^{17}O > 0$ occurs at high-temperatures by $H + SiO_2 \rightarrow OH + SiO$, followed by $OH + H_2 \rightarrow H_2O + H$. McSween (1977) found that CAIs are about 5% by volume of carbonaceous chondrites, with values ranging from 0.3% in Renazzo to 9.4% in Allende. The elemental abundances within CAIs have been demonstrated to be close to solar when sampling biases are properly accounted for (Simon and Grossman, 2004). The photospheric ratios of Ca/Si and Al/Si are 0.065 and 0.042, respectively (Lodders, 2003), suggesting that a solar fraction of CAIs would be ~ 5% of the total silicate fraction in the solar nebula. Isotopic mass balance requires that the SiO_2 produced in scheme II (center downward branch) would have a positive $\Delta^{17}O$ with a magnitude ~ 1/20 of $\Delta^{17}O$(CAIs), or ~ $+1‰$, comparable to the $\Delta^{17}O$ values measured in ordinary chondrites (e.g., McKeegan and Leshin, 2001). Nebular water in isotopic equilibrium with silicates will have a positive $\Delta^{17}O$, but a factor of 2–3 lower, demonstrating that chemical MIF as outlined in scheme II cannot account for the Choi et al. (1998) and Sakamoto et al. (2007) observations, at least when applied to a solar gas.

Enhancement of dust relative to gas will increase $\Delta^{17}O$ of silicates and water in the chemical MIF scenario. Conservation of $\Delta^{17}O$ for the solar nebula in the vicinity of CAI formation may be written as

$$\Delta^{17}O(\text{neb}) \approx \beta f_{\text{CAI}}\Delta^{17}\text{O(CAI)} + \beta f_{sil}\Delta^{17}\text{O}(sil) + f_{\text{CO+H}_2\text{O}}\Delta^{17}\text{O(CO + H}_2\text{O)} \approx 0,$$

where f_i is the atom fraction of oxygen for component i relative to bulk solar composition (taken from Lodders, 2003), and β is the dust enrichment factor relative to solar gas silicate (i.e., the enrichment of Si, Mg, Fe, Ca, Al, etc., relative to the amount condensed from a gas of solar composition). Ca and Al are assumed to be exclusively in CAIs, but CAIs also contain some Mg and Si. The amount of Mg and Si in CAIs was taken from the average of all CAI bulk compositions reported by Grossman et al. (2008). The remaining Mg and Si (most of it) and all of the Fe is assumed to be in silicates. For CAIs and silicates, the amount of oxygen is one atom per atom of Mg, Fe and Ca, 1.5 atoms per atom of Al and 2 atoms per atom of Si. Using the abundances of Lodders (2003), we calculate the following fi values: $f_{CO+H2O} = 5.3 \times 10^{-4}$, $f_{sil} = 1.4 \times 10^{-4}$ and $f_{CAI} \sim 1.2 \times 10^{-5}$. For no dust enhancement ($\beta = 1$), and assuming isotopic equilibration of silicates, CO and H_2O, we find $\Delta^{17}O(CO + H_2O) = \Delta^{17}O(\text{silicate}) = +0.90‰$. For higher dust enrichment ($\beta >> 10$), we find that $\Delta^{17}O(CO + H_2O) = \Delta^{17}O(\text{silicate}) = 4.3‰$.

These $\Delta^{17}O$ values for high-temperature CO, H_2O and silicate are too low by a factor of ~2 compared to the nebular water $\Delta^{17}O$ values inferred from carbonaceous chondrites (Clayton and Mayeda, 1984; Young, 2001) and magnetite measurements (Choi et al., 1998), and are a factor of ~20 below the recent values inferred from Acfer 094 matrix (Sakamoto et al., 2007). The size of the water reservoir represented by the Acfer 094 results is unclear; it may be negligible compared to bulk nebular water. Nevertheless, if the chemical MIF mechanism is to account for the observed oxygen isotopes in both CAIs and nebular water, some modification to the surface MIF mechanism (Marcus, 2004) appears to be necessary.

5. THE SURFACE NEBULA

CO self-shielding at the nebular surface (region 3 of Fig. 1) was previously discussed (Thiemens and Heidenreich, 1983; Navon and Wasserburg, 1985; Lyons, 2002), but was first treated quantitatively by Lyons and Young (2005a) (LY05). Thiemens and Heidenreich rejected O_2 self-shielding as unimportant in an H_2-rich nebular environment. However, Kitamura and Shimizu (1983) showed that at temperatures of ~100 K H_2O photolysis would lead to O_2 in the nebular surface. Kitamura and Shimizu proposed that mineral grains would exchange oxygen with ^{17}O and ^{18}O-enriched O atoms produced from O_2 photolysis during shock events. They also suggested that planetesimals would have formed from these isotopically enriched grains. However, Kitamura and Shimizu did not discuss the isotopic composition of the Sun, which is a necessary test of self-shielding models. Although Kitamura and Shimizu (1983) did not account for O atom exchange with O_2, which will act to erase an O_2-derived isotope effect (Navon and Wasserburg, 1985), they did identify several key aspects of present-day self-shielding theories.

Here, we will focus on quantitative models for CO self-shielding We will not review LY05 in detail, but will instead show some of the results from that model that were not included in the original publication; all of these results have been presented (by J.R.L.) at conferences since 2004. LY05 utilized a 1-D atmospheric chemistry code (courtesy of J. Kasting), adapted to the solar nebula, to account for turbulent vertical mixing of all chemical species, including oxygen isotopologues. The model assumes a 2-D minimum-mass solar nebula (MMSN) with an α-viscosity

parameterization of turbulent mixing, and also assumes that the vertical diffusivity, D, is identical to the radial turbulent viscosity, v. (The validity of the latter assumption is discussed below.) The chemical reactions in the model are derived from a subset of the UMIST database of reactions (Le Teuff et al., 2000) and include gas–grain reactions on the surfaces of dust grains (Willacy et al., 1998). An example of δ-values for several species in the model illustrating the very large fractionations that occur, especially in the early stages of photolysis, is shown in Fig. 3.

Several timescales relevant to the α-disk model are shown in Fig. 4. The maximum positive $\Delta^{17}O$ for total nebula H_2O occurs when ~ ½ of the column abundance of CO is dissociated. However, this maximum $\Delta^{17}O$ is also a function of the intensity of the radiation field, G_0, and of α. The timescale $t_{surf\ CO}$ is defined, at a given radial distance, as the shortest time needed to reach the inferred $\Delta^{17}O$ for bulk nebular H_2O, as inferred from carbonaceous chondrites (Clayton and Mayeda, 1984; Young, 2001). At 30 AU the shortest $t_{surf\ CO}$ is $\sim 10^5$ years (Fig. 4) for $\alpha \sim 10^{-2}$ and $G_0 \sim 10^3$, which is comparable to the diffusive radial transport timescale, t_{radial}, at 30 AU. As discussed in LY05 self-shielding of surface CO can yield a significant fraction of ^{16}O-depleted H_2O at the midplane of a MMSN only if vertical mixing is rapid ($D = \alpha > 10^{-3}$). Weak mixing ($\alpha \sim 10^{-4}$ or less) precludes reaching the inferred $\Delta^{17}O$ values in nebular water (Fig. 5). Similarly, at heliocentric distances <10–20 AU, $t_{surf\ CO}$ becomes comparable to the expected lifetime of the nebular gas (few My) (Fig. 6). A recent box model of the solar nebula (Young, 2007), emphasizing radiation from the protosun rather than from a nearby massive star, yields similar CO photodissociation timescales ($\sim 10^5$ years) at similar distances (~30 AU). (As a point of clarification, the Young (2007) model is not an extension of the model developed by Lyons in LY05. The two sets of calculations are independent.)

A few additional points concerning self-shielding at the nebular surface must be made. First, dust provides a surface for condensation of H_2O vapor, with eventual sequestration of ice-coated dust at the midplane. Dust evolution by growth and sedimentation is intimately tied to the availability of surface area for condensation. In LY05 dust was assumed to be static and uniformly distributed. One of us (J.R.L.) is presently extending the photochemical model to include dust evolution (Ciesla, 2007). These results will be coupled to a radial transport model (Ciesla and Cuzzi, 2006). Second, the nebular surface (region 3, Fig. 1) is very likely to be MRI-active. Dust sedimentation here will be fast ($t_{surf\ sed}$, Fig. 4), and a reservoir of ^{16}O-enriched CO will be present (Fig. 7). The ^{16}O-enriched reservoir will move inward with a smaller diffusive timescale than the bulk outer nebula because $\alpha_3 > \alpha_4$, where the subscripts refer to the re-

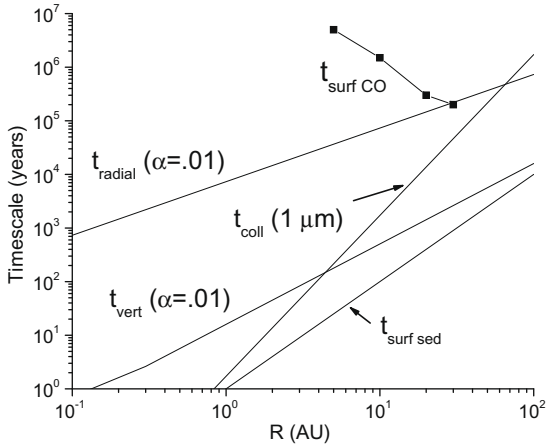

Fig. 4. Several timescales as a function of heliocentric distance in the solar nebula (MMSN). The radial and vertical diffusive timescales, t_{radial} and t_{vert}, are computed for $\alpha = 10^{-2}$. The collision timescale, t_{coll}, is the time between collisions of uniformly distributed 1 μm dust particles, assuming a gas to dust ratio of 100. $t_{surf\ CO}$ is the time required to photolyze ~ ½ of the total column of CO at a given heliocentric distance, assuming an interstellar radiation field.

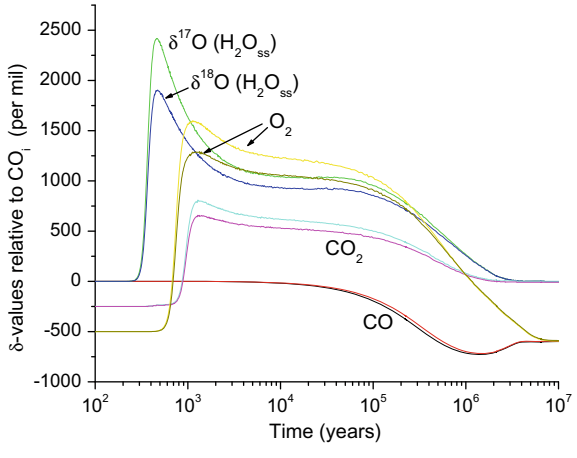

Fig. 3. Delta values for several constituents of a solar nebula model at a heliocentric distance of 30 AU, at the disk midplane, $\alpha = 10^{-2}$ and $G_0 = 500$. H_2O_{ss} is water produced from O liberated during CO photolysis. Very large delta values are predicted at early times.

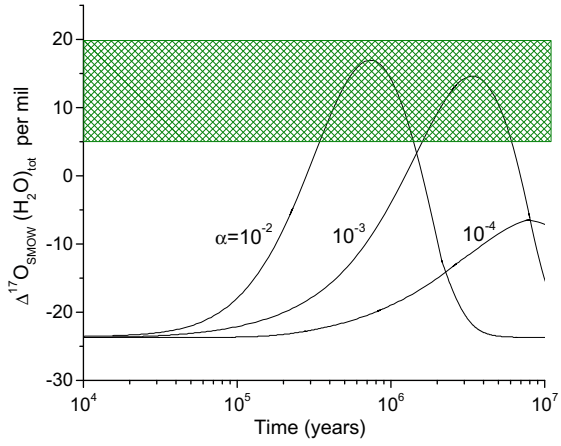

Fig. 5. $\Delta^{17}O$ of total nebula H_2O as a function of time at 30 AU and for $G_0 = 500$. Weak mixing, a viscosity parameter $\alpha \sim 10^{-4}$, leads to $\Delta^{17}O(H_2O)$ values below that inferred to have been present from carbonaceous chondrites (hatched area).

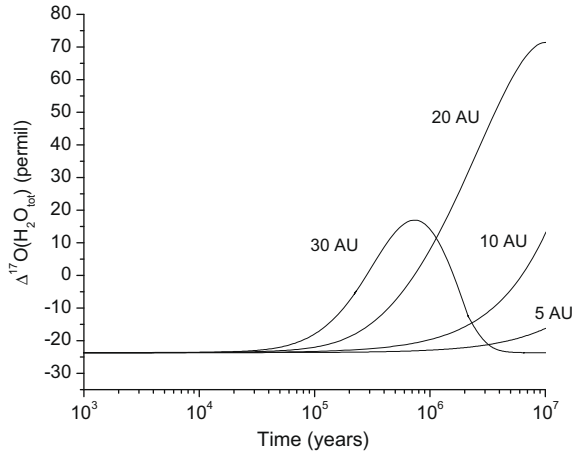

Fig. 6. $\Delta^{17}O$ of total nebula H_2O as a function of heliocentric distance for $\alpha = 10^{-2}$ and $G_0 = 500$. The lifetime of nebular gas (few My) requires $\Delta^{17}O(H_2O)$ be formed at distances >10 AU.

gions in Fig. 1. Mixing between the surface region and the top of dead zone is weak but nonzero, and will transfer this ^{16}O-enriched reservoir into the much more massive dead zone. Such pockets of ^{16}O-rich CO may transfer their isotope signature to dead zone silicates during shock events (Kitamura and Shimizu, 1983), and could provide a mechanism to explain extreme ^{16}O-rich chondrules (Kobayashi et al., 2003). Third, the nebular gas temperature may be elevated relative to the dust temperature in the zone of active CO photodissociation (e.g., Jonkheid et al., 2004) because of photoelectric effect on polycyclic aromatic hydrocarbons (PAHs) and H_2 formation. Evidence for elevated gas temperatures comes from observations of rotational temperatures in a variety of disk surface molecules. In AA Tau rotational temperatures from 350–900 K have been measured inside of 3 AU (Carr and Najita, 2008). Although grains and gas are not in thermal equilibrium in the surface disk (>4 scale heights above the midplane), an elevated gas

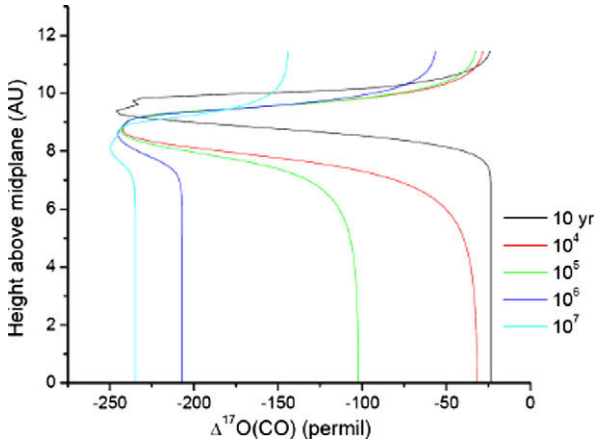

Fig. 7. Model profiles of $\Delta^{17}O$ of CO at 30 AU for $\alpha = 10^{-2}$ and $G_0 = 500$. At early times ($<10^5$ years) $\Delta^{17}O(CO) << 0$ is concentrated in the surface layers of the disk.

temperature heats grain surfaces and increases the rate of desorption of ice from the grain. An increased rate of desorption increases the fraction of H_2O as vapor, and leads to more rapid conversion of H_2O back to CO via H_2O photolysis and subsequent reactions with C-containing ions and molecules. The importance of these processes needs to be explored quantitatively in the surface shielding models.

LY05 showed that as $C^{17}O$ and $C^{18}O$ are preferentially photodissociated and the liberated O atoms react with H_2 to form water, $\Delta^{17}O(H_2O)$ rises, approaching several percent. Then, as the ^{16}O-poor water reacts with other species and chemical equilibrium is established, $\Delta^{17}O$ falls. In order for an isotopic signature to be preserved and transferred to solar nebula solids, the ^{16}O-poor water must be vertically mixed to the disk midplane before this chemical equilibrium is established. The rate of chemical equilibrium scales roughly as the UV flux (parameterized via G_0), and the rate of vertical mixing scales roughly as the degree of turbulence in the disk (parameterized via α). Generally speaking, isotopically fractionated water will reach the meteorites only if G_0 and α are both "high" or both "low". In what follows, we use the timescales of the problem to constrain the values of these parameters.

Calculations in LY05 reveal the timescales over which isotopic fractionation in water are produced. They assume a MMSN at 30 AU and a midplane temperature of 51 K. The diffusion coefficient of vertical mixing was set equal to $\alpha H^2 \Omega$, with $\alpha = 10^{-2}$. The scale height of the disk is $H = c/\Omega$, where c is the sound speed and Ω the Keplerian orbital frequency. Fig. 2 of LY05 shows two trends. First, the timescale over which isotopic fractionations are established scales inversely with the UV flux. For $G_0 \sim 5$ the timescales are several My, while for $G_0 \sim 10^3$ they peak at about 0.2 My, and for $G_0 \sim 10^4$ they peak at just about 0.1 My. Second, the peak fractionation also scales inversely with G_0. As long as $G_0 < 10^4$, the peak fractionations pass through the required range ($\Delta^{17}O = +5‰$ to $+20‰$) at some point. Significantly, the fractionation of water tends to linger in this range for the longest time (for $\sim 4 \times 10^5$ y) if $G_0 \sim 10^3$. Faster timescales obtain if a higher effective α characterizes the vertical diffusion. These results are robust in the sense that many disk configurations (G_0 and α) potentially can explain the observed oxygen isotope fractionations in meteorites. For an effective $\alpha \sim 10^{-2}$, the models suggest $G_0 \sim 10^3$–10^4. These UV fluxes are consistent with those expected in high-mass star-forming regions (see Section 3). We now discuss the likely magnitude of turbulent diffusion.

The cause of turbulent diffusion in disks is almost certainly the magnetorotational instability, or MRI (Balbus and Hawley, 1991). Essentially the only requirements are that a large-scale magnetic field threads the disk, and that the ionization fraction is high enough locally for the gas to couple to the magnetic field. In protoplanetary disks the ionization fraction is likely to exceed the threshold in the surface layers everywhere due to the combination of low densities and unattenuated X-ray and galactic cosmic ray ionization. The delineation between these actively accreting layers and the MRI-stable "dead zones" is, however, sensitive to the disk structure

and the ionization chemistry. Here we make some estimates of the boundary between the active layers and dead zones. In the context of the Hayashi minimum-mass solar nebula, surface densities are $\Sigma(r) = 10\ (r/30\ \mathrm{AU})^{-1.5}\ \mathrm{g\ cm^{-3}}$. In the Desch (2007) model they are only somewhat higher at these radii: $\Sigma(r) = 32\ (r/30\ \mathrm{AU})^{-2.2}\ \mathrm{g\ cm^{-3}}$. A necessary (but not sufficient) requirement for initiating the MRI is that the ionization fraction exceed a critical value of $10^{-13}\ (T/100\ \mathrm{K})^{-0.5}\ r^{-1.5}$, where r is the radius in AU (Gammie, 1996), to overcome the electrical resistivity of the gas. This critical ionization fraction is only exceeded outside of 10 AU in the Hayashi et al. (1985) model, and outside of 20 AU using the Desch (2007) surface density. These predictions of the radial extent of the dead zones are consistent with other more sophisticated models (Sano et al., 2000). Beyond these radii, the stability of the disk is likely to be sensitive to more subtle effects such as the degree of Hall diffusion (Wardle, 1999; Desch, 2004). In what follows we adopt the picture of dead zones overlain by actively accreting layers, extending out to beyond 30 AU.

In the active, MRI-unstable layers of the disk, the turbulent viscosity reaches levels $v \sim \alpha H^2 \Omega$, with α estimated from numerical simulations to be at least 10^{-3}, potentially as high as 0.5, depending on the disk conditions. Pessah et al. (2007) recently reviewed the results of 35 modeling papers that estimated the value of α in MRI-turbulent disks. They found that the majority of simulations were affected by numerical limitations and derived a simple formula for α. In a realistic disk in which the MRI has progressed to a steady state (so that the magnetic field strength has grown to about 0.1 times the equipartition field), it is straightforward to show that α approaches 0.5. This is consistent with constraints from a variety of observations of dwarf novae, X-ray transients and active galactic nuclei disks, which are all fully ionized and for which values $\alpha \approx 0.1$–0.4 are inferred.

Within the dead zones α is much lower than in the active layers, but is not zero. With ratios of dead zone surface densities to active layer densities ~10, Fleming and Stone (2003) and Oishi et al. (2007) found dead zone $\alpha \sim 10^{-4}$–10^{-5}. If the active layer is active because of X-ray ionization, a reasonable estimate of the surface density is a few $\mathrm{g\ cm^{-2}}$ (Igea and Glassgold, 1999), which is roughly one tenth of the total surface density in the disk and the dead zone at 30 AU, $\sim 30\ \mathrm{g\ cm^{-2}}$. Clearly further modeling is necessary to verify these estimates, but they suggest an active layer with $\alpha \sim 0.1$ and surface density $3\ \mathrm{g\ cm^{-2}}$, and a dead zone with $\alpha \sim 3 \times 10^{-4}$ and surface density $30\ \mathrm{g\ cm^{-2}}$. Transport in this disk is dominated by the active layer, and a vertically integrated α (weighted by mass) yields $\alpha \sim 10^{-2}$ in the context of radial transport.

Observations of radial spreading of protoplanetary disks support an effective $\alpha \sim 10^{-2}$. Models of the disk evolution around DM Tau and GM Aur imply $\alpha \sim 10^{-2}$ (Hueso and Guillot, 2005). Likewise Hartmann et al. (1998) model the viscous spreading of disks in low-mass star-forming regions with $\alpha \sim 10^{-2}$. The combined weight of the evidence then is that the outer regions of disks may be divided into dense dead zones and thin active layers a few $\mathrm{g\ cm^{-2}}$ thick.

The turbulent viscosity is related to the diffusivity of gases via the Schmidt number, $Sc = v/D$, where D is the diffusion coefficient. Numerical simulations (Johansen et al., 2006) show that for mixing in the vertical direction, $Sc = 8.8\ (\alpha/0.1)^{0.46}$, while for mixing in the radial direction, $Sc = 2.5\ (\alpha/0.1)^{0.26}$. In other words, if $\alpha = 0.1$, mixing in the vertical direction is equivalent to an effective value $\alpha \approx 0.01$, and radial mixing equivalent to $\alpha = 0.04$ within the active layer, vertically averaged to $\alpha = 0.004$. Disk photoevaporation has been neglected in modeling of nebular mixing and surface nebular CO self-shielding. For $G_0 \sim 10^3$–10^4 photoevaporation of the disk occurs on timescales ~3–10 My at 47 AU in an MMSN (Adams et al., 2004), and is even longer at 30 AU. The CO photodissociation timescales are ~0.1–1 My at 30 AU, and even shorter at larger heliocentric distances, and so are rapid compared to disk evaporation.

The rate of mixing by MRI-induced turbulence is exactly in line with the values of α favored by the chemical model. The chemical model described above assumed vertical mixing with effective $\alpha = 10^{-2}$. At 30 AU, the vertical mixing timescale is $\approx 1/(\alpha\ \Omega) \approx 2000$ y. The radial mixing timescale is $\approx (r/H)^2\ /\ (\alpha\ \Omega) \sim 1$ My, which is comparable to the timescales for producing the isotopic fractionations if $G_0 = 10^3$–10^4, and comparable to the timescales for disk evolution. Closer to the Sun, the radial mixing timescale falls steeply with r (roughly as r^2), so that even though α is expected to decrease nearer the Sun (due to the presence of dead zones), the bottleneck for radial mixing would probably remain the 30 AU region. We therefore conclude that isotopically fractionated water can be transported effectively to the inner regions of the disk, by turbulent diffusion.

6. SELF-SHIELDING IN THE PARENT CLOUD

External radiation fields can create anomalies via isotopic selective photodissociation on the disk surface (Lyons and Young, 2005a) or on the surface of the molecular cloud that condensed to form the Sun (Yurimoto and Kuramoto, 2004). In the latter case, Yurimoto and Kuramoto (2004) presented the schematic outline and justification for anomaly creation in molecular clouds by considering astronomical observations and model simulations on cloud surfaces, and by pointing out the key role played by water ice concentration in the disk midplane following cloud collapse. Lee et al. (2008) explored the creation of anomalies in a detailed model of cloud collapse. This model utilizes information gleaned from our current astronomical understanding of the physics and chemistry of collapse of condensed regions—called cores—within molecular clouds (e.g., Lee et al., 2004) coupled to a model of the oxygen isotope production as outlined in Lyons and Young (2005a). A key feature of this new model is the capability to explore the external environment of the solar nebula. Most stars in the Galaxy are formed in stellar clusters with associated massive stars (Lada and Lada, 2003). These massive stars are strong emitters of molecule destroying ultraviolet radiation that lie at the heart of the new schemes for production of oxygen isotope enhancements. Hence, it is probable that

the Sun formed in a cluster and its natal core was exposed to a radiation field that is enhanced when compared to the average interstellar radiation field.

Lee et al. (2008) model the collapsing cloud as inside-out collapse of an 10 K isothermal sphere, within which isotopic selective photodissociation produces an atomic oxygen layer near the exposed core surface where ^{18}O and ^{17}O are enhanced relative to ^{16}O. These oxygen atoms then freeze onto cold grain surfaces and form water ice on the grain surface via catalytic reactions with atomic hydrogen. Water ice is strongly bound to grain surfaces and these enhancements are maintained throughout the subsequent evolution until the gas/dust mixture is carried close to the newly forming star (~several AU). Some key results of the model can be summarized. (1) Very large isotopic anomalies are produced on the cloud surface depending on the strength of the external radiation field ($\delta^{18}O_{SMOW} \sim \delta^{17}O_{SMOW}$ ~50−1000‰; we use SMOW as a reference for comparison with meteorites), comparable to and larger than recent inferred δ-values for nebular water (Sakamoto et al., 2007). (2) These anomalies can be carried inward by collapse to the protoplanetary disk. Within the disk the "surface" ices will be mixed with ices produced without anomalies deeper inside the cloud (Yurimoto and Kuramoto, 2004). (3) To create meteoritic anomalies the gas and ice-coated dust motions within the disk must be decoupled to some extent (e.g., Kuramoto and Yurimoto, 2005; Ciesla and Cuzzi, 2006). (4) Because the mass of the cloud is large, it is possible to seed the entire disk with oxygen isotope enhancements that can later be incorporated into solids. In addition, the isotope ratio of the forming Sun can also be slightly altered and is dependent on the strength of the external radiation field. An accurate measurement of the solar oxygen isotope ratio as inferred from solar wind (McKeegan et al., 2008a,b) may provide a strong constraint on the external environment in which the Sun formed (this is true for both surface nebular shielding and parent cloud shielding models). By contrast, surface shielding models are not capable of influencing the oxygen isotope composition of the Sun. The best estimate of solar oxygen isotope ratio presently available (McKeegan et al., 2008b) suggests that the Sun formed in an environment where the ultraviolet radiation field was enhanced and that the Sun therefore formed within a cluster of stars including at least one star that is significantly more massive (>5 solar masses). The Lee et al. (2008) model corroborates the suggestion of Yurimoto and Kuramoto (2004), and demonstrates the strong dependence of the resulting H_2O ice δ-values on the radiation field (and time) at the inner edge (~100 AU) of the collapsing cloud (Fig. 8).

Rapid inward transport of high $\Delta^{17}O$ water ice along the disk surface (e.g., Ciesla, 2007) may have supplied the water necessary to form the high $\Delta^{17}O$ phases observed in Acfer 094 (Sakamoto et al., 2007). Alternatively, and perhaps assisted by photodesorption and photolysis in the disk surface layer, the high $\Delta^{17}O$ water ice may have undergone low temperature (i.e., <300 K) reaction with accreted grains in the vicinity of the accretion shock. Watson et al. (2007) have recently observed water emission from a low mass (~0.14 $M_\odot$) class 0 protoplanetary disk. They infer a gas temperature of ~170 K from far-infrared emission lines. This temperature is consistent with accretion onto a protoplanetary disk, as Watson et al. argue, but is not high enough to drive isotopic reequilibration of H_2O and CO (Lyons and Young, 2005b). Isotopic reequilibration could occur via photochemical reactions in the accretion zone in which H_2O is dissociated and reacts with C and O radicals and ions, but the high observed dust opacity makes this unlikely. Observations of higher mass disks exhibiting water emission may prove to be more directly comparable to the early solar nebula.

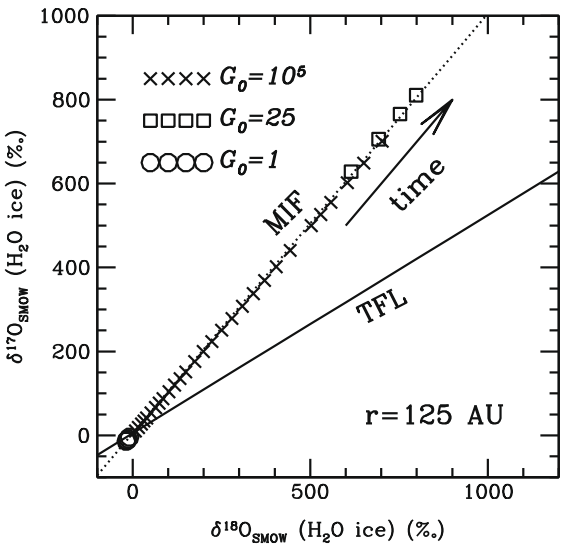

Fig. 8. δ-Values for H_2O ice formed from CO in a collapsing cloud core. Results are shown at 125 AU, which is the inner boundary of the collapsing cloud model, and for several values of G_0, which defines the intensity of the interstellar radiation field. The plotted values start at the time of completion of solar accretion (0.45 My). Each symbol corresponds to a timestep of 50 Kyr for $G_0 = 1$ and 25, and 5 Kyr for $G_0 = 10^5$. The large δ-values predicted for H_2O ice may be the source of high $\Delta^{17}O$ phases present in Acfer matrix (Sakamoto et al., 2007). By definition, $\delta^{17}O = \delta^{18}O$ for CO self-shielding in the model. (Figure from Lee et al. (2008) with permission of *Meteoritics & Planetary Science*, © 2008 by the Meteoritical Society.)

7. RADIAL TRANSPORT OF OXYGEN ISOTOPES

Currently, in all models for the CAI mixing line, the location of the isotopic fractionation is very different from the regions where the terrestrial planets and meteorite parent bodies are expected to form. Specifically, the chondritic meteorites, which preserve the original isotopic composition of the nebular solids that were accreted into the building blocks of the planets, are thought to have formed at the midplane of the nebula between 2 and 4 AU. The mechanisms discussed thus far have focused solely on producing a nebular component that is enriched in heavy oxygen (water) from a solar composition (presumed to have $\delta^{17,18}O = -50‰$). Two further steps are thus required: transport of these anomalies to the region where terrestrial materials formed and isotopic exchange between the isotopically heavy water and silicate minerals.

The exact order in which these additional steps are thought to take place depends on the particular model for self-shielding being discussed. In the model of Clayton (2002), self-shielding takes place at the very inner edge of the solar nebula (<0.1 AU) where high-temperatures are expected, thus allowing isotopic exchange between nebular silicates and nebular water to take place in the same region. In this region, dissociation of CO leads to far more oxidizing conditions than thermodynamic equilibrium for a solar composition gas, such that iron-bearing silicates can condense at high-temperature (Clayton, 2005). Such a region may also be the location from which protostellar jets are launched (Shu et al., 1996). If this is the case, both the solids and gas present in this region could be launched in the X-wind, with the gas being carried out to space, possibly with small dust grains entrained. Larger solids, however, will eventually decouple from the gas, or potentially be launched on ballistic trajectories which carries them both upward and away from the central star. These solids would then rain back down upon the solar nebula, where they could be incorporated into growing planetesimals. An advantage of this mechanism as proposed is that the high-temperature processing of chondrules and CAIs and their redistribution throughout the nebula are explained by a single process. A disadvantage of this mechanism is that matrix is considered to be ambient nebular material not heated by close proximity to the protosun (Shu et al., 1996), a supposition not supported by the chemical and isotopic similarity of matrix to chondrules.

In the models of Yurimoto and Kuramoto (2004) (hereafter, YK04) and LY05, the situation is more complex. These models predict that water becomes enriched in heavy oxygen either in the molecular cloud from which the solar system formed (YK04) or at the surface of the nebula in the cool, outer regions far from the star (LY05). The low temperatures of these environments allow for more efficient trapping of the isotope anomaly in water ice, however these temperatures are well below those that are needed to allow for isotopic exchange between the water and silicates that would be present. These low temperatures are necessary to prevent complete erasure of the isotopic fractionation through recombination of the liberated oxygen with the carbon atom to which it was bonded. At these low temperatures, if the oxygen atom collides with a silicate grain, it can stick to its surface, provided its encounter velocity was low. The oxygen atom can then bond with hydrogen on the grain surface to form H_2O. Once this isotopically heavy water has formed, it is necessary to transport it to a region of the nebula in which temperatures are high enough for such exchange to take place. Oxygen exchange may also occur during passage of nebular shock waves. With water ice concentrated near the midplane relative to CO gas, isotope exchange will form more ^{16}O-depleted silicates.

Solids, such as water ice, are subjected to three major forms of transport in the solar nebula: diffusion due to turbulence, advective flows, and gas drag migration. Turbulence is likely tied to the evolution of the solar nebula, that is, the transport of mass through the nebula and onto the Sun. The cause of this evolution is still the subject of ongoing research, with the two leading candidates being a viscosity ($v = \alpha cH$) produced through the magnetorotational instability (Balbus and Hawley, 1991) or gravitational torques (e.g., Boss, 2002; Boley et al., 2006). Under steady-state conditions, the large-scale advective flow of the disk has a local velocity of $V_r = -v/2r$ (typical velocities are 0.01–1 m s^{-1}) and the diffusion coefficient of a tracer-species is given by $D \sim v$ (i.e., $Sc \sim 1$). Gaseous molecules in the disk are also subjected to both of these forms of transport. In the hot inner solar nebula X-winds and/or disk winds may also be an important form of transport for nonvolatile grains, and are invoked in Clayton (2002), but will not be quantitatively considered here.

The model of solar nebula evolution put forth by Desch (2007) suggests an outward flow of mass through the outer solar system (a few to 30 AU) during the era of planet formation, beginning soon (few $\times 10^5$ y) after the disk is first exposed to an external UV flux, and continuing for as long as 10 My. As the model of Desch (2007) favors $\alpha \approx 4 \times 10^{-4}$, the timescale for outward transport is several My; by necessity, this is comparable to the inward mixing of material by diffusion. Inward transport of isotopically fractionated gas should proceed in any case, but at a marginally reduced rate (factors of a few).

Gas drag migration of solids arose due to the radial pressure gradient that was present in the solar nebula (hot, dense gas close to the Sun and cool, sparse gas further out). This pressure gradient served to partially support the gas against the gravity of the Sun, effectively reducing the central force, and allowing the gas to orbit the Sun at sub-Keplerian rates. Solids in the nebula would not feel this pressure gradient, and thus would attempt to orbit the Sun at Keplerian velocities. The motion of the solids through the gas resulted in a drag force on the solids, causing them to lose energy and angular momentum to the gas and spiral inwards over time. Weidenschilling (1977) found that the inward drift rate was a strong function of size, with meter-sized bodies drifting inwards at the highest rate of speed ($\sim$50 m s^{-1}).

These dynamic processes that could have combined with water derived from CO self-shielding to produce the oxygen isotope variations seen in chondritic meteorites. Water ice in the outer solar nebula would have been incorporated into larger and larger bodies through collision and sticking processes with other solids. As these solids grew, they drifted inwards more rapidly than the isotopically lighter gas due to gas drag migration, meaning the inward flux of heavy oxygen isotopes would exceed the inward flux of the light isotopes.

As the icy solids drifted inwards, they would eventually cross the snow line. Upon entering this warmer region of the nebula, the water would be released from the solids and be incorporated into the gas. While this gas then will continue to move inwards due to the advective flows in the disk, it will do so at a much slower rate than it is delivered by the icy solids migrating inward from the outer disk. This leads to a "pile up" of water vapor, where the local concentration can exceed the solar value. Cuzzi and Zahnle (2004) originally estimated that this pile up would result in concentrations of water that were 100–1000 times solar.

More detailed models by Ciesla and Cuzzi (2006) found that the finite mass of the disk limited the enhancements to being <10 times solar. While temperatures just inside the snow line would still be too low to allow for isotopic exchange between the water and silicates, energetic events such as those responsible for chondrule formation would allow such exchange to take place.

In the YK04 model, it is the level of water enhancement that determines the magnitude in the shift of the oxygen isotope values in chondritic materials. In this model, the water is globally enriched in heavy oxygen prior to the formation of the solar nebula, and thus the average $\delta^{17,18}O$ values (averaged over silicates, water, and CO) of a gas of solar composition would be equivalent to that of the parent molecular cloud, expected to be $-50‰$. However, by preferentially increasing the concentration of the isotopically heavy water, the average $\delta^{17,18}O$ would become higher. Yurimoto and Kuramoto (2004) estimated that water enhancements of 2–5 would be sufficient to produce the observed range of oxygen isotope ratios, consistent with the migration models of Ciesla and Cuzzi (2006). The water in the LY05 model may require a lower level of water enhancement in the inner solar nebula because the water produced as a result of self-shielding in the outer solar nebula is delivered to the inner nebula before the isotopically light CO arrives. In the YK04 model inner nebula CO is already isotopically enriched in ^{16}O when the outer solar system water arrives. Both models require some level of water enrichment.

The YK04 and LY05 models are intriguing as they tie the evolution of the oxygen isotopes to the dynamical evolution of water in the solar nebula. Not only would the abundance of water vapor in the inner solar system affect the oxygen isotopic ratios seen in chondritic materials, but it would also affect the redox state of the nebula, and thus the specific mineralogy of what is able to form (e.g., Kuramoto and Yurimoto, 2005). CAIs, whose mineralogies suggest that they formed in a gas of solar composition (Yoneda and Grossman, 1995) also record the most ^{16}O-rich formation environment. Chondrules and processed matrix, which are enriched in heavy isotopes of oxygen by comparison, appear to have formed in a wide range of redox conditions, with the high levels of FeO observed in ordinary and carbonaceous chondrites requiring very oxidizing conditions to form (e.g., enhanced water concentrations; Krot et al., 2000) whereas the enstatite chondrites require very reducing conditions (depleted water concentrations relative to solar) to explain the incorporation of Si into the Fe-metal and other minerals unique to that class of meteorite (Cyr et al., 1999; Hutson and Ruzicka, 2000). The enstatite chondrites precursor materials may have been processed in the ^{16}O-depleted inner nebula along with other silicate materials, and then processed a second time in a more reducing, water-depleted nebula. Given that dynamical models predict both enhancements and depletions of the water vapor in the inner solar nebula (Cuzzi and Zahnle, 2004; Ciesla and Cuzzi, 2006), the YK04 and LY05 models offer a way of simultaneously explaining the chemical and isotopic composition of chondrules and matrix, including the enstatite chondrites. Transport models predict that water depletion in the inner nebula should occur ~1 My after water enhancement, which should be reflected in a younger formation age for the enstatite chondrites if this scenario is correct.

8. TIMESCALES OF OXYGEN ISOTOPE EXCHANGE

The self-shielding scenarios (YK04; LY05) in which ^{16}O-depleted water is transported from the outer solar nebula to inside the snow line require oxygen isotope exchange between nebular water and silicates (chondrules and matrix). It is most likely that this exchange occurred between nebular gas and chondrules during chondrule formation events, rather than in low temperature aqueous alteration. The timescales for diffusion of oxygen in CAI mineral grains and hot chondrules may be used to assess the viability of this process. We use the laboratory data from Ryerson and McKeegan (1994) on diffusion in CAIs, Oishi et al. (1974) on CAS melts, and Yu et al. (1995) on chondrule melts. The diffusion timescale in a spherical grain of diameter a is $t_{diff} \sim a^2/4D$, where $D = D_0 e^{-Q/RT}$ is the diffusion coefficient and Q is the activation energy for diffusion. Diffusion timescales as a function of temperature for grains with $a = 1$ mm are given in Fig. 9. This calculation neglects surface kinetic effects (Yu et al., 1995) and assumes CAIs of a single mineral composition.

Chondrule formation is believed to occur by shock heating (e.g., Desch and Connolly, 2002; Ciesla and Hood, 2002). Peak temperatures of 1800–2100 K are maintained for several minutes, largely melting the chondrule and most CAI precursors. Cooling occurs on a range of timescales (~10–100 K hr^{-1}), but is largely complete within ~1 day or less. Fig. 9 shows that the oxygen diffusion timescale in

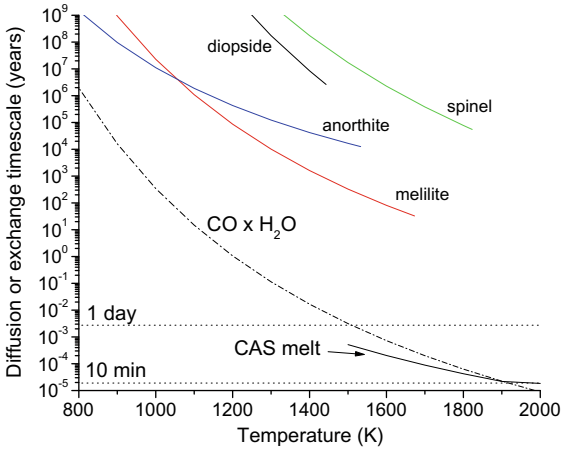

Fig. 9. Computed timescales for oxygen diffusion in several CAI minerals (Ryerson and McKeegan, 1994) and Ca–Al–silicate melt (Oishi et al., 1974). The timescale curves stop at the mineral condensation temperatures determined for the components of typical type B CAIs (Stolper, 1982). All diffusion calculations assume a 1 mm diameter spherical grain. Also shown is the timescale for exchange between CO and H_2O in the nebular at a total pressure of 10^{-3} bars. The timescales of peak chondrule heating (<10 min) and more gradual chondrule cooling (~1 day) are indicated by dotted lines.

a 1 mm sample of CAS melt at peak heating temperatures is comparable to or less than the duration of heating, which argues for complete exchange. Diffusion in 1 mm diameter spinel minerals is $\sim 10^9$ times slower at 1800 K. Thus, shock heating of large spinel grains (condensed from a solar gas ~1 My earlier, probably close to the X-point) and chondrule precursors in the 1–3 AU region of the nebula is consistent with preferential exchange of (^{16}O-depleted) nebular oxygen with chondrules. Integrated heating times of $\sim 10^2$ – 10^3 years at 1600 K estimated from Mg isotopes (Young et al., 2005; Young, 2007) argue for greater oxygen exchange in melilite and negligible exchange in spinel, as is observed in CAIs (McKeegan and Leshin, 2001). However, many CAI and chondrule components will be melted simultaneously under strong shock heating conditions, so that exchange would be expected for both sets of precursor grains. Apart from spinel, the very simple analysis (e.g., partial melting is neglected) presented in Fig. 9 does not support the preferential gas–chondrule exchange versus gas–CAI exchange. Exchange of oxygen between CO and H_2O gases in the nebula is rapid (Fig. 9) compared to gas–solid exchange (Alexander, 2004). Preferential exchange of silicate melt with H_2O versus CO (Boesenberg et al., 2005) may be important for moderate heating events, depending on the size of the melt droplets.

9. TESTS OF THE THEORIES

The models discussed in this paper can be used to make testable predictions. For the grain surface chemical mass-independent fractionation theory of Marcus (2004), the most important test is laboratory demonstration of the effect. By contrast, the self-shielding theories invoke an effect known to occur, but for which accurate quantification is not yet possible. The self-shielding models propose that CO shielding occurred in one or more of three distinct locations (parent cloud, nebular surface, X-point). The temperature and pressure dependence of CO photochemical fractionation at these locations can in principle be used to determine the best model. Accurate temperature-dependent CO photodissociation calculations are needed for this to be a meaningful test, but require accurate CO isotopologue cross section data. An essential test of the self-shielding scenario is to determine whether fractionation with a slope near unity does in fact occur when all bands of CO are accounted for. The experimental results of Chakraborty et al. (2008) on selected subsets of bands show significant wavelength dependence in O isotope fractionation, but are not able to address the net fractionation due to broadband radiation.

Can we distinguish among the three self-shielding models? All three models invoke isotopic modification (i.e., ^{16}O-depletion) of the terrestrial planet-forming region of the solar nebula. The surface disk model and the parent cloud model predict that the giant planets are also isotopically enriched (e.g., Yurimoto et al., 2007), unless Jupiter formed faster than the timescale for surface self-shielding (<<1 My), in which case Jupiter may be solar in oxygen isotopes if surface shielding was dominant. Because the oxygen isotopic compositions of most planets, with the exception of Earth, Moon and Mars, are unknown, we cannot rule out self-shielding models on the basis of planetary oxygen isotopes. The discovery of large ^{16}O-depletion in Acfer 094 grains (Sakamoto et al., 2007) will likely provide a useful constraint to the self-shielding models, particularly models that include radial transport. It is possible that the Acfer 094 data is not consistent with X-point self-shielding, due to reduced isotope fractionation at high-temperatures, but this requires further investigation. For now we must use careful evaluation of the self-shielding models, together with new CO cross section data, to determine which (if any) of the models is correct. Such modeling should be supplemented by observations of other young stellar objects to constrain the physical and chemical conditions (e.g., Carr and Najita, 2008) and possibly isotopic composition (e.g., Smith et al., 2008) of nebular gas in protoplanetary disks.

Other isotope systems such as H, C and N isotopes, may offer additional tests of the self-shielding theory. Each of these has only 2 stable isotopes, and so unambiguous MIF signatures are not possible, but large photochemically induced isotope signatures may still be recognized. We will consider C and N isotopes here, but not discuss H isotopes which undergo large isotope fractionation due to numerous processes. C produced by CO photolysis will be isotopically enriched due to self-shielding, and the residual CO will be depleted in ^{13}C. Carbon atoms are ionized in roughly the same wavelength range in which CO is photolyzed, and so C atoms are rapidly converted to C^+ ions and higher order organics species. Carbon-13 ions undergo rapid and slightly exothermic exchange with ^{12}CO, $^{12}CO + {}^{13}C^+ \leftrightarrow {}^{13}CO + {}^{12}C^+ + 35$ K, which leads to ^{13}C enrichment of CO in the cold disk midplane. A recent MMSN disk model (Woods and Willacy, 2009) obtains δ^{13}C values for CO of $\sim -40‰$ to $-150‰$ in the disk surface and positive thousands of ‰ in the midplane inward of 30 AU. Because most disk organic compounds (e.g., H_2CO, CH_4, HCN, etc.) are derived from C^+, the model predicts ^{12}C-enriched organics in the cold midplane, in good agreement with observations of HCN in Comet Hale-Bopp (Jewitt et al., 1997). The disk model of Woods and Willacy considers CO and H_2 dissociation due only to a ~1 G_0 interstellar radiation field, and does not include vertical mixing, both of which limit comparison with the type of solar nebula discussed here. Nevertheless, their model clearly demonstrates the importance of ^{13}C fractionation due to ion-molecule exchange at low temperatures. Hashizume et al. (2004) likewise proposed a test for the formation pathway of planetary carbon by comparing the carbon isotopic ratio of the solar composition and the planetary composition represented by those of the bulk meteoritic organics. They have pointed out a slight enhancement of ^{13}C for the planetary composition based on the solar wind carbon composition observed among lunar grains, however, verification of the solar composition is necessary for further discussion.

N_2 self-shielding is also very likely in a nebula and/or parent cloud environment. The discovery of massive ^{15}N enrichment in lithic clasts in CB and CH carbonaceous

chondrites (Sugiura et al., 2000; Ivanova et al., 2008) could be due to either low temperature ion-molecule chemistry that leads to NH_3 formation (Charnley and Rodgers, 2002; Rodgers and Charnley, 2008) or N2 self-shielding. N2 is isoelectronic with CO and has a series of bands qualitatively similar to CO from 91 to 100 nm. Liang et al. (2007) have demonstrated that N_2 self-shielding yields large isotopic fractionation in the upper atmosphere of Titan, where product N atoms are rapidly converted to HCN. Similar reactions are expected in the outer solar nebula and parent cloud to form HCN and other products, which form ices on grains at rates qualitatively similar to H_2O ice. Reaction of HCN with other organics compounds could yield refractory organics that would be effectively transported into the inner solar system and incorporated into CB and CH parent bodies or matrix material. One of us (J.R.L.) derived approximate N_2 shielding functions from the Liang et al. (2007) model, and incorporated them in the LY05 disk model. Using a restricted set of nitrogen reactions (including HCN but not NH_3), large ^{15}N fractionation is predicted, particularly at very early times (Fig. 10). These results needs to be verified with a more complete chemical model, but do demonstrate N_2 self-shielding is potentially important in the disk, and also in the parent cloud. Whether N_2 self-shielding modified the nitrogen isotopic composition of the bulk solar nebula, or at least the inner solar nebula as proposed by Clayton (2002), is less clear. Nitrogen isotopes in TiN refractory grains (Meibom et al., 2007) have $\delta^{15}N$ values similar to Jovian NH_3 (Owen et al., 2001) and to upper limits from analyses of lunar grains (Hashizume et al., 2000), all of which are depleted in ^{15}N relative to chondrites and the terrestrial planets. The ^{15}N enrichment of bulk chondrites and terrestrial planets may be in part a result of N_2 self-shielding.

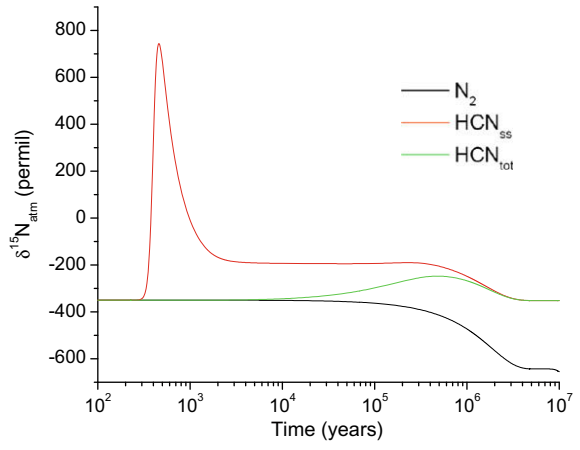

Fig. 10. Model results for the nitrogen isotopic composition of HCN ice produced from N_2 photodissociation. Self-shielding in N_2 yields an enrichment in ^{15}N atoms. N_2 shielding functions were estimated from a Titan atmospheric model (Liang et al., 2007). Results shown are for the nebula midplane at 30 AU, and assume $\alpha = 0.01$ and an isothermal disk temperature of 51 K. The initial isotopic composition of N_2 is assumed to be $-350‰$ relative to the terrestrial atmosphere (subscript 'atm'). Only about 30 nitrogen reactions have been included in this preliminary model.

10. CONCLUSIONS

We have focused on two models for the CAI mixing line: 1) CO self-shielding and 2) chemical mass-independent fractionation. The two models we have focused on make distinct predictions for the oxygen isotope composition of the Sun. CO self-shielding models predict that the Sun is depleted in ^{17}O and ^{18}O by $\sim 50‰$ relative to SMOW (Clayton, 2002). Chemical MIF models predict that the Sun is $\sim 0‰$ relative to SMOW (Marcus, 2004; Thiemens, 2006). The location of the anomalous isotope fractionation also differs between these models. Chemical MIF occurs during CAI formation, and requires the constituents of CAIs be present in the gas phase. This requirement implies temperatures above that of silicate sublimation (>1400 K), and therefore chemical MIF is restricted to regions of the nebula that are hotter than the dust front (i.e., generally at radii less than the dust front) but below the temperatures of CAI condensation. By contrast CO self-shielding has been proposed at three locations: (1) the hot inner solar nebula (Clayton, 2002), (2) the outer nebular surface (LY05), and 3) the precollapse cloud core (YK04; Lee et al., 2008). Preliminary Genesis results (McKeegan et al., 2008b) provide evidence for an isotopically light solar wind, consistent with CO self-shielding (Clayton, 2002), but not necessarily at the X-point. The next step is to quantitatively constrain the primary location at which the self-shielding occurred. Model results from Lyons and Young (2005a) and Lee et al. (2008) demonstrate the need for a high FUV environment ($G_0 \sim 10^3$ or more), consistent with formation of the solar system in a stellar cluster consisting of at least hundreds of stars.

The self-shielding models, together with radial transport models of the nebula, inherently contain several important timescales that can be related to the evolution of chondrites (e.g., Krot et al., 2005). Radial transport timescales are $\sim$0.1–1 My for $\alpha \sim 0.01$–0.001, respectively, from the outer nebula. This defines the transport timescale for ^{16}O-depleted water, produced by CO self-shielding at either the outer nebular surface or in the parent cloud, into the inner solar system, and is consistent with the age difference measured for CAIs and chondrules (e.g., Amelin et al., 2002). Surface self-shielding requires that a substantial fraction of the CO initially present in the nebula is converted to H_2O and organics (LY05). Radiation fields of $\sim 10^2$–10^4 G_0 yield optimal CO dissociation and H_2O production in the outer nebula on timescales of 0.1–1 My. CO self-shielding in the parent cloud can yield large abundances of highly ^{16}O-depleted H_2O for a wide range of radiation fields (Lee et al., 2008), including $G_0 \sim 10^3$–10^5. The surface self-shielding model is most consistent with an interstellar radiation field expected for a cluster of $\sim 10^3$ stars; radiation from the central star is also potentially important but the necessary 2-D radiative transfer problem has not been properly solved yet. The general picture of CO self-shielding due to radiation in a medium-to-large-sized cluster may be consistent with injection of ^{60}Fe from a nearby supernova, and with photoevaporative truncation of the outer disk to the orbits of KBOs ($\sim$47 AU).

In order for a self-shielding scenario to be viable, CAIs must reside within the (presumably inner) solar nebula for ~1 My until the time of chondrule formation. In addition, after the ^{16}O-depleted water has arrived from the outer solar system, chondritic silicates must undergo oxygen isotope exchange due to either the ambient temperature of the nebular gas, or to sporadic heating events from protosolar flares and/or other nebular shocks, whereas the most refractory CAIs must resist exchange. Condensation of CAIs from a high pressure (up to ~0.1 atm) solar gas (Grossman et al., 2008) is consistent with formation in the vicinity of the X-point. The X-wind could have transported the CAIs to the meteorite-forming region of the nebula. CAIs, chondrules and matrix material underwent (probably episodic) heating, and chondrules and matrix exchanged oxygen isotopes with nebular H_2O, but CAIs did not. The timescales for oxygen isotope diffusion in melted chondrules are ~ minutes (Yu et al., 1995), whereas the oxygen diffusion timescales in unmelted spinel (1 mm diameter) is ~1–10^5 years (Ryerson and McKeegan, 1994) at temperatures corresponding to chondrule formation. Most other CAI minerals are likely to have melted under chondrule formation conditions, and therefore will have undergone oxygen exchange. Grain size and partial melting considerations must be included in an analysis of the relative degree of chondrule and CAI mineral exchange with the nebular gas. Enstatite chondrite precursors were comprised of ^{16}O-depleted silicates, but appear to have been processed a second time in a highly reducing environment. Such an environment is consistent with the arrival of water-depleted gas from the outer solar system on timescales of ~2 My, although obtaining sufficient water enhancement to deplete bulk silicates in ^{16}O at times <1 My and sufficient water depletion at later times to form enstatite chondrites may be problematic (Ciesla and Cuzzi, 2006).

In the X-point version of self-shielding (Clayton, 2002), all inner solar system CAIs and silicates pass through the X-point. Silicates exchange oxygen isotopes with nebular ^{16}O-depleted H_2O gas, but CAIs do not. The younger age of chondrules is more difficult to accommodate in this theory because of the more nearly simultaneous formation and transport of CAIs and chondrules. If a reservoir of ^{16}O-depleted H_2O can be transported and maintained at ~2–4 AU by the X-wind, it may be possible to form (or reform) chondrules much later than CAIs, perhaps by nebular shocks generated by the formation of Jupiter ~1 My after the formation of CAIs.

ACKNOWLEDGMENTS

The authors thank the reviewers (H. Yurimoto, M. Chaussidon and an anonymous reviewer) and the associate editor (A. Krot) for their thorough reviews and numerous comments and suggestions that greatly improved the paper. J.R.L. thanks K. McKeegan, D. Burnett, and A. Kallio for discussions of the preliminary oxygen analyses of Genesis samples, and R. Clayton for discussions on various topics. This work was supported by the NASA Origins Program (J.R.L., S.J.D.) and the NASA Cosmochemistry Program (A.M.D.). F.J.C. acknowledges support from NASA's Discovery Data Analysis Program. J.-E. Lee gratefully acknowledges funding from the Korea Science and Engineering Foundation (KOSEF) to the Astrophysical Research Center for the Structure and Evolution of the Cosmos (ARCSEC).

REFERENCES

Adams F. C. and Laughlin G. (2001) Constraints on the birth aggregate of the solar system. *Icarus* **150**, 151–162.

Adams F. C., Hollenbach D., Laughlin G. and Gorti U. (2004) Photoevaporation of circumstellar disks due to external far-ultraviolet radiation in stellar aggregates. *Astrophys. J.* **611**, 360–379.

Alexander C. M. O'D. (2004) Chemical equilibrium and kinetic constraints for chondrule and CAI formation conditions. *Geochim. Cosmochim. Acta* **68**, 3943–3969.

Amelin Y., Krot A. N., Hutcheon I. D. and Ulyanov A. A. (2002) Lead isotopic ages of chondrules and calcium–aluminum-rich inclusions. *Science* **297**, 1678–1683.

Balbus S. A. and Hawley J. F. (1991) A powerful local shear instability in weakly magnetized disks. I. Linear analysis. *Astrophys. J.* **376**, 214–233.

Bally J. and Langer W. D. (1982) Isotope-selective photodissociation of carbon monoxide. *Astrophys. J.* **255**, 143–148.

Boesenberg J. S., Young E. D., Ziegler K. and Hewins R. H. (2005) Evaporation and the absence of oxygen isotope exchange between silicate melt and carbon monoxide gas at nebular pressures. *Meteorit. Planet. Sci.* **40**, A22.

Boley A. C., Mejía A. C., Durisen R. H., Cai K., Pickett M. K. and D'Alessio P. (2006) The thermal regulation of gravitational instabilities in protoplanetary disks. III. Simulations with radiative cooling and realistic opacities. *Astrophys. J.* **651**, 517–534.

Boss A. P. (2002) Evolution of the solar nebula. V. Disk instabilities with varied thermodynamics. *Astrophys. J.* **576**, 462–472.

Carr J. S. and Najita J. R. (2008) Organic molecules and water in the planet formation region of young circumstellar disks. *Science* **319**, 1504–1506.

Chakraborty S., Ahmed M., Jackson T. L. and Thiemens M. H. (2008) Experimental test of self-shielding in vacuum ultraviolet photodissociation of CO. *Science* **321**, 1328–1331.

Charnley S. B. and Rodgers S. D. (2002) The end of interstellar chemistry as the origin of nitrogen in comets and meteorites. *Astrophys. J.* **569**, L133–L137.

Choi B.-G., McKeegan K. D., Krot A. N. and Wasson J. T. (1998) Extreme oxygen-isotope compositions in magnetite from unequilibrated ordinary chondrites. *Nature* **392**, 577–579.

Ciesla F. L. and Hood L. L. (2002) The nebular shock wave model for chondrule formation: Shock processing in a particle–gas suspension. *Icarus* **158**, 281–293.

Ciesla F. J. (2007) Dust coagulation and settling in layered protoplanetary disks. *Astrophys. J.* **654**, L159–L162.

Ciesla F. J. and Cuzzi J. N. (2006) The evolution of the water distribution in a viscous protoplanetary disk. *Icarus* **181**, 178–204.

Clayton D. D. (1988) Isotopic anomalies: chemical memory of galactic evolution. *Astrophys. J.* **334**, 191–195.

Clayton R. N. (2002) Self-shielding in the solar nebula. *Nature* **415**, 860–861.

Clayton R. N. (2005) Disequilibrium oxygen chemistry in the solar nebula. *Lunar Planet. Sci. XXXVI*, #1711 (CD-ROM).

Clayton R. N., Grossman L. and Mayeda T. K. (1973) Component of primitive nuclear composition in carbonaceous meteorites. *Science* **182**, 485–488.

Clayton R. N. and Mayeda T. K. (1984) The oxygen isotope record in Murchison and other carbonaceous chondrites. *Earth Planet. Sci. Lett.* **67**, 151–161.

Cuzzi J. N. and Zahnle K. J. (2004) Material enhancement in protoplanetary nebulae by particle drift through evaporation fronts. *Astrophys. J.* **614**, 490–496.

Cyr K. E., Sharp C. M. and Lunine J. I. (1999) Effects of the redistribution of water in the solar nebula on nebular chemistry. *Journal Geophys. Res.* **104**, 19003–19014.

Davis A. M., Hashizume K., Chaussidon M., Ireland T. R., Allende Prieto C. and Lambert D. (2008) Oxygen in the Sun. *Rev. Mineral. Geochem.* **68**, 73–92.

Desch S. J. and Connolly, Jr., H. C. (2002) A model of the thermal processing of particles in solar nebula shocks: Application to the cooling rates of chondrules. *Meteorit. Planet. Sci.* **37**, 183–207.

Desch S. J. (2004) Linear analysis of the magnetorotational instability, including ambipolar diffusion, with application to protoplanetary. *Astrophys. J.* **608**, 509–525.

Desch S. J. (2007) Mass distribution and planet formation in the solar nebula. *Astrophys. J.* **671**, 878–893.

Dullemond C. P., Dominik C. and Natta A. (2001) Passive irradiated circumstellar disks with an inner hole. *Astrophys. J.* **560**, 957–969.

Eidelsberg M., Sheffer Y., Federman S. R., Lemaire J. L., Fillion J. H., Rostas F. and Ruiz J. (2006) Oscillator strengths and predissociation rates for Rydberg transitions in 12C16O, 13C16O, and 13C18O involving the E1Π, B1Σ+, and W 1Π states. *Astrophys. J.* **647**, 1543–1548.

Elmegreen B. G. and Efremov Y. N. (1997) A universal formation mechanism for open and globular clusters in turbulent gas. *Astrophys. J.* **480**, 235–245.

Fatuzzo M. and Adams F. C. (2008) UV radiation fields produced by young embedded star clusters. *Astrophys. J.* **675**, 1361–1375.

Fleming T. and Stone J. M. (2003) Local magnetohydrodynamic models of layered accretion disks. *Astrophys. J.* **585**, 908–920.

Gammie C. F. (1996) Layered accretion in T Tauri disks. *Astrophys. J.* **457**, 355–362.

Gao Y. Q. and Marcus R. A. (2001) Strange and unconventional isotope effects in ozone formation. *Science* **293**, 259–263.

Gao Y. Q. and Marcus R. A. (2002) On the theory of strange and unconventional isotopic effects on ozone formation. *J. Chem. Phys.* **116**, 137–154.

Gao Y. Q. and Marcus R. A. (2007) An approximate theory of the ozone isotopic effects: rate constant ratios and pressure dependence. *J. Chem. Phys.* **127**(244316/), 1–8.

Gounelle M. and Meibom A. (2007) The oxygen isotopic composition of the Sun as a test of the supernova origin of ^{26}Al and ^{41}Ca. *Astrophys. J.* **664**, L123–L125.

Gounelle M. and Meibom A. (2008) The origin of short-lived radionuclides and the astrophysical environment of solar system formation. *Astrophys. J.* **680**, 781–792.

Grossman L. (1972) Condensation in primitive solar nebula. *Geochim. Cosmochim. Acta* **36**, 597–619.

Grossman L., Ebel D. S., Simon S. B., Davis A. M., Richter F. M. and Parsad N. M. (2000) Major element chemical and isotopic compositions of refractory inclusions in C3 chondrites: the separate roles of condensation and evaporation. *Geochim. Cosmochim. Acta* **64**, 2879–2894.

Grossman L., Simon S. B., Rai V. K., Thiemens M. H., Hutcheon I. D., Williams R. W., Galy A., Ding T., Fedkin A. V., Clayton R. N. and Mayeda T. K. (2008). *Geochim. Cosmochim. Acta* **72**, 3001–3021.

Hartmann L., Calvet N., Gullbring E. and D'Alessio P. (1998) Accretion and the evolution of T Tauri disks. *Astrophys. J.* **495**, 385–400.

Hashizume K., Chaussidon M., Marty B. and Robert F. (2000) Solar wind record on the Moon: deciphering presolar from planetary nitrogen. *Science* **290**, 1142–1145.

Hashizume K., Marty B. and Wieler R. (2002) Analyses of nitrogen and argon in single lunar grains: towards a quantification of the asteroidal contribution to planetary surfaces. *Earth Planet. Sci. Lett.* **202**, 201–216.

Hashizume K., Chaussidon M., Marty B. and Terada K. (2004) Protosolar carbon isotopic composition: implications for the origin of meteoritic organics. *Astrophys. J.* **600**, 480–484.

Hashizume K. and Chaussidon M. (2005) A non-terrestrial ^{16}O-rich isotopic composition for the protosolar nebula. *Nature* **434**, 619–622.

Hashizume K. and Chaussidon M. (2008) Evidence of at least two extra-selenial components accreting on the Moon—In search for the oxygen isotopic composition of the solar component trapped in lunar metal grains. *Lunar Planet. Sci. XXXIX*, #1531 (CD-ROM).

Hayashi C., Nakazawa K. and Nakagawa Y. (1985) Formation of the solar system. In *Protostars and Planets III* (eds. J. I. Lunine and E. Levy). University of Arizona Press, Tucson, pp. 1100–1153.

Hester J. J. and Desch S. J. (2005) Understanding our origins: star formation in H II region environments. In *Chondrites and the Protoplanetary Disk. ASP Conference Series*, Vol. 341 (eds. A. N. Krot, E. R. D. Scott and B. Reipurth). Astronomical Society of the Pacific, San Francisco, pp. 107–130.

Hueso R. and Guillot T. (2005) Evolution of protoplanetary disks: constraints from DM Tauri and GM Aurigae. *Astron. Astrophys.* **442**, 703–725.

Hutson M. and Ruzicka A. (2000) A multi-step model for the origin of E3 (enstatite) chondrites. *Meteorit. Planet. Sci.* **35**, 601–608.

Ida S., Larwood J. and Burkert A. (2000) Evidence for early stellar encounters in the orbital distribution of Edgeworth–Kuiper Belt objects. *Astrophys. J.* **528**, 351–356.

Igea J. and Glassgold A. E. (1999) X-Ray ionization of the disks of young stellar objects. *Astrophys. J.* **518**, 848–858.

Ireland T. R., Holden P., Norman M. D. and Clarke J. (2006) Isotopic enhancements of 17O and 18O from solar wind particles in the lunar regolith. *Nature* **440**, 776–778.

Ireland T. R., Holden P., Norman M. D., Mya J.and Asplund M. (2007) Soils ain't soils: the preservation of solar wind in metal grains from the lunar regolith. *Lunar Planet. Sci. XXXVII*, #1449 (CD-ROM).

Ivanova M. A., Konokova N. N., Krot A. N., Greenwood R. C., Franchi I. A., Verchovsky A. B., Trieloff M., Korochantseva E. V. and Brandstatter F. (2008) The Isheyevo meteorite: Mineralogy, petrology, bulk chemistry, oxygen, nitrogen, carbon isotopic compositions and 40Ar-39Ar ages. *Meteoritics Planet. Sci.* **43**, 915–940.

Jacobsen B., Yin Q.-Z., Moynier F., Amelin Y., Krot A. N., Nagashima K., Hutcheon I. D. and Palme H. (2008) ^{26}Al–^{26}Mg and 207Pb–206Pb systematics of Allende CAIs: canonical solar initial ^{26}Al/^{27}Al ratio reinstated. *Earth Planet. Sci. Lett.* **272**, 353–364.

Jewitt D. C., Matthews H. E., Owen T. and Meier R. (1997) Measurements of 12C/13C, 14N/15N, and 32S/34S ratios in Comet Hale-Bopp (C/1995 O1). *Science* **278**, 90–93.

Johansen A., Klahr H. and Mee A. J. (2006) Turbulent diffusion in protoplanetary discs: the effect of an imposed magnetic field. *Mon. Not. Royal Astron. Soc.* **370**, L71–L75.

Jonkheid B., Faas F. G. A., van Zadelhoff G.-J. and van Dishoeck E. F. (2004) The gas temperature in flaring disks around pre-main sequence stars. *Astron. Astrophys.* **428**, 511–521.

Kenyon S. J. and Bromley B. C. (2004) Stellar encounters as the origin of distant solar system objects in highly eccentric orbits. *Nature* **432**, 598–602.

Kitamura Y. and Shimizu M. (1983) Oxygen isotope anomaly and solar nebular photochemistry. *Moon and Planets* **29**, 199–202.

Kobayashi S., Imai H. and Yurimoto H. (2003) New extreme ^{16}O-rich reservoir in the early solar system. *Geochem. J.* **37**, 663–669.

Krot A. N., Fegley, Jr., B., Lodders K. and Palme H. (2000) Meteoritical and astrophysical constraints on the oxidation state of the solar nebula. In *Protostars and Planets IV* (eds. V. Mannings, A. P. Boss and S. S. Russell). University of Arizona Press, Tucson, pp. 1019–1054.

Krot A. N., McKeegan K. D., Leshin L. A., MacPherson G. J. and Scott E. R. D. (2002) Existence of an ^{16}O-rich gaseous reservoir in the solar nebula. *Science* **295**, 1051–1054.

Krot A. N., Hutcheon I. D., Yurimoto H., Cuzzi J. N., McKeegan K. D., Scott E. R. D., Libourel G., Chaussidon M., Aléon J. and Petaev M. I. (2005) Evolution of oxygen isotopic composition in the inner solar nebula. *Astrophys. J.* **622**, 1333–1342.

Krot A. N., Amelin Y., Bizzarro M., Bland P., Ciesla F. J., Connelly J., Davis A. M., Huss G. R., Hutcheon I. D., Makide K., Nagashima K., Russell S. S., Scott E. R. D., Thrane K., Yurimoto H. and Yin Q.-Z. (2009) Origin and chronology of chondritic components: a review. *Geochim. Cosmochim. Acta* **73**, 4963–4997.

Kuramoto K. and Yurimoto H. (2005) Oxygen isotopic heterogeneity in the solar system: the molecular cloud origin hypothesis and its implications for meteorites and the planets. In *Chondrites and the Protoplanetary Disk. ASP Conference Series 341* (eds. A. N. Krot, E. R. D. Scott and B. Reipurth). Astronomical Society of the Pacific, San Francisco, pp. 181–192.

Lada C. J. and Lada E. A. (2003) Embedded clusters in molecular clouds. *Ann. Rev. Astron. Astrophys.* **41**, 57–115.

Laughlin G. and Adams F. C. (1998) The modification of planetary orbits in dense open clusters. *Astrophys. J.* **508**, L171–L174.

Lee J.-E., Bergin E. A. and Evans, II, N. J. (2004) Evolution of chemistry and molecular line profiles during protostellar collapse. *Astrophys. J.* **617**, 360–383.

Lee J.-E., Bergin E. A. and Lyons J. R. (2008) Oxygen isotope anomalies of the Sun and the original environment of the solar system. *Meteorit. Planet. Sci.* **43**, 1351–1362.

Le Teuff Y. H., Millar T. J. and Markwick A. J. (2000) The UMIST database for astrochemistry 1999. *Astron. Astrophys. Suppl. Ser.* **146**, 157–168.

Liang M. C., Heays A. N., Lewis B. R., Gibson S. T. and Yung Y. L. (2007) Source of nitrogen isotope anomaly in HCN in the atmosphere of Titan. *Astrophys. J.* **664**, L115–L118.

Lodders K. (2003) Solar system abundances and condensation temperatures of the elements. *Astrophys. J.* **591**, 1220–1247.

Lyons J. R. (2002) Self-shielding of CO and the oxygen isotope anomaly in meteorites: Unique clues to conditions in the very young solar system. *Astrobiology* **2**, 532.

Lyons J. R. and Young E. D. (2005a) CO self-shielding as the origin of oxygen isotope anomalies in the early solar nebula. *Nature* **435**, 317–320.

Lyons J. R. and Young E. D. (2005b) Photochemical speciation of oxygen isotopes in the Solar Nebula. In *Chondrites and the Protoplanetary Disk. ASP Conference Series 341* (eds. A. N. Krot, E. R. D. Scott and B. Reipurth). Astronomical Society of the Pacific, San Francisco, pp. 193–211.

Lyons J. R., Boney E. and Marcus R. A. (2008) Self-shielding at the X-point in the E(1)-X(0) band of CO. *Lunar Planet. Sci. XXXIX*, #2265 (CD-ROM).

Marcus R. A. (2004) Mass-independent isotope effect in the earliest processed solids in the solar system: a possible mechanism. *J. Chem. Phys.* **121**, 8201–8211.

Marcus R. A. (2008) Mass-independent oxygen isotope fractionation in selected systems. Mechanistic considerations. *Adv. Quant. Chem.* **55**, 5–19.

Mauersberger K., Erbacher B., Krankowsky D., Gunther J. and Nickel R. (1999) Ozone isotope enrichment: isotopomer-specific rate coefficients. *Science* **283**, 370–372.

McKeegan K. D. and Leshin L. A. (2001) Stable isotope variations in extraterrestrial materials. *Rev. Mineral. Geochem.* **43**, 279–318.

McKeegan K. D., Jarzebinski G., Kallio A. P., Mao P. H., Coath C. D., Kunihiro T., Wiens R., Allton J., Callaway M., Rodriguez M. and Burnett D. S. (2008a) A first look at oxygen in a Genesis concentrator sample. *Lunar Planet. Sci. XXXIX*, #2020 (CD-ROM).

McKeegan K. D., Coath C. D., Heber, V., Jarzebinski G., Kallio A. P., Kunihiro T., Mao P. H. and Burnett D. S. (2008b) The oxygen isotopic composition of captured solar wind: first results from the Genesis. *EOS Trans*. AGU 89(53), *Fall Meet*. Suppl., P42A-07 (abstr.).

McSween, Jr., H. Y. (1977) Petrographic variations among carbonaceous chondrites of the Vigarano type. *Geochim. Cosmochim. Acta* **41**, 1777–1790.

Meibom A., Krot A. N., Robert F., Mostefaoui S., Russell S., Petaev M. I. and Gounelle M. (2007) Nitrogen and carbon isotopic composition of the Sun inferred from a high-temperature solar nebular condensate. *Astrophys. J.* **656**, L33–L36.

Navon O. and Wasserburg G. J. (1985) Self-shielding in O2—A possible explanation for oxygen isotope anomalies in meteorites? Earth Planet. *Sci. Lett.* **73**, 1–16.

Oishi Y., Terai R. and Ueda H. (1974) Oxygen diffusion in liquid silicates and relation to their viscosity. In *Mass Transport in Ceramics* (eds. A. R. Cooper and A. H. Heuer). Plenum Press, pp. 297–310.

Oishi J. S., Mac Low M. M. and Menou K. (2007) Turbulent torques on protoplanets in a dead zone. *Astrophys. J.* **670**, 805–819.

Owen T., Mahaffy P. R., Niermann H. B., Aytreya S. and Wong M. (2001) Protosolar nitrogen. *Astrophys. J.* **553**, L77–L79.

Pessah M. E., Chan C.-K. and Psaltis D. (2007) Angular momentum transport in accretion disks: scaling laws in MRI-driven turbulence. *Astrophys. J.* **668**, L51–L54.

Rodgers S. D. and Charnley S. B. (2008) Nitrogen superfractionation in dense cloud cores. *Mon. Notic. Roy. Astron. Soc.* **385**, L48–L52.

Ryerson F. J. and McKeegan K. D. (1994) Determination of oxygen self-diffusion in ikermanite, anorthite, diopside, and spinel: Implications for oxygen isotopic anomalies and the thermal histories of Ca–Al-rich inclusions. *Geochim. Cosmochim. Acta.* **58**, 3713–3734.

Sakamoto N., Seto Y., Itoh S., Kuramoto K., Fujino K., Nagashima K., Krot A. N. and Yurimoto H. (2007) Remnants of the early solar system water enriched in heavy oxygen isotopes. *Science* **317**, 231–233.

Sano T., Miyama S. M., Umebayashi T. and Nakano T. (2000) Magnetorotational instability in protoplanetary disks. II. Ionization state and unstable regions. *Astrophys. J.* **543**, 486–501.

Seto Y., Sakamoto N., Fujino K., Kaito T., Oikawa T. and Yurimoto H. (2008) Mineralogical characterization of a unique material having heavy oxygen isotope anomaly in matrix of the primitive carbonaceous chondrite Acfer 094. *Geochim. Cosmochim. Acta* **72**, 2723–2734.

Shu F., Shang H. and Lee T. (1996) Toward an astrophysical theory of chondrites. *Science* **271**, 1545–1552.

Simon S. B. and Grossman L. (2004) A preferred method for the determination of bulk compositions of coarse-grained refractory inclusions and some implications of the results. *Geochim. Cosmochim. Acta* **68**, 4237–4248.

Smith R. L., Pontoppidan K. M., Young E. D., Morris M. R. and van Dishoeck E. F. (2008) Detection of rare CO isotopologues in protostellar disks: an infrared investigation of molecular self shielding. *Workshop on Chronology of Meteorites, Kauai*, November 5–7, 4073 (abstr.).

Stolper E. (1982) Crystallization sequences of Ca–Al inclusions from Allende: An experimental study. *Geochim. Cosmochim. Acta* **46**, 2159–2180.

Sugiura N., Zashu S., Weisberg M. and Prinz M. (2000) A nitrogen isotope study of bencubbinites. *Meteorit. Planet. Sci.* **35**, 987–996.

Thiemens M. H. and Heidenreich, III, J. E. (1983) The mass-independent fractionation of oxygen—A novel isotope effect and its possible cosmochemical implications. *Science* **219**, 1073–1075.

Thiemens M. H. (1988) Heterogeneity in the nebula: evidence from stable isotope. In *Meteorites and the Early Solar System* (eds. J. F. Kerridge and M. S. Matthews). University of Arizona Press, Tucson, pp. 899–923.

Thiemens M. H. (1999) Mass-independent isotope effects in planetary atmospheres and the early solar system. *Science* **283**, 341–345.

Thiemens M. H. (2006) History and applications of mass-independent isotope effects. *Annu. Rev. Earth Planet. Sci.* **34**, 217–262.

Trujillo C. A. and Brown M. E. (2001) The radial distribution of the Kuiper Belt. *Astrophys. J.* **554**, L95–L98.

Wadhwa M., Amelin Y., Davis A. M., Lugmair G. W., Meyer B., Gounelle M. and Desch S. J. (2007) From dust to planetesimals: Implications for the solar protoplanetary disk from short-lived radionuclides. In *Protostars and Planets V* (eds. B. Reipurth, D. Jewitt and K. Keil). University of Arizona Press, Tucson, pp. 835–848.

Wardle M. (1999) The Balbus–Hawley instability in weakly ionized discs. *Mon. Not. Roy. Astron. Soc.* **307**, 849–856.

Wasserburg G. J., Busso M. and Gallino R. (1996) Abundances of actinides and short-lived nonactinides in the interstellar medium: Diverse supernova sources for the r-processes. *Astrophys. J.* **466**, L109–L113.

Watson D. M., Bohac C. J., Hull C., Forrest W. J., Furlan E., Najita J., Calvet N., D'Alessio P., Hartmann P. L., Sargent B., Green J. D., Kim K. H. and Houck J. R. (2007) The development of a protoplanetary disk from its natal envelope. *Nature* **448**, 1026–1028.

Weidenschilling S. J. (1977) Aerodynamics of solid bodies in the solar nebula. *Mon. Not. Royal Astron. Soc.* **180**, 57–70.

Wieler R., Humbert H. and Marty B. (1999) Evidence for a predominantly non-solar origin of nitrogen in the regolith revealed by single grain analyses. *Earth Planet. Sci. Lett.* **167**, 47–60.

Wiens R. C., Neugebauer M., Reisenfeld D. B., Moses, Jr., R. W., Nordholt J. E. and Burnett D. S. (2003) Genesis solar wind concentrator: computer simulations of performance under solar wind conditions. *Space Sci. Rev.* **105**, 601–625.

Willacy K., Klahr H. H., Millar T. J. and Henning Th. (1998) Gas and grain chemistry in a protoplanetary disk. *Astron. Astrophys.* **338**, 995–1005.

Woods P. M. and Willacy K. (2009) Carbon isotope fractionation in protoplanetary disks. *Astrophys. J.* **693**, 1360–1378.

Yoneda S. and Grossman L. (1995) Condensation of CaO–MgO–Al_2O_3–SiO_2 liquids from cosmic gases. *Geochim. Cosmochim. Acta* **59**, 3413–3444.

Young E. D. (2001) The hydrology of carbonaceous chondrite parent bodies and the evolution of planet progenitors. *Phil. Trans. R. Soc. Lond. A* **359**, 2095–2110.

Young E. D., Simon J. I., Galy A., Russell S. S., Tonui E. and Lovera O. (2005) Supra-canonical $^{26}Al/^{27}Al$ and the residence time of CAIs in the solar protoplanetary disk. *Science* **308**, 223–227.

Young E. D. (2007) Time-dependent oxygen isotopic effects of CO self shielding across the solar protoplanetary disk. *Earth Planet. Sci. Lett.* **262**, 468–483.

Young E. D., Kuramoto K., Marcus R. A., Yurimoto H. and Jacobsen S. B. (2008) Mass-independent oxygen isotope variation in the solar nebula. *Rev. Mineral. Geochem.* **68**, 187–218.

Yu Y., Hewins R. H., Clayton R. N. and Mayeda T. K. (1995) Experimental study of high temperature oxygen isotope exchange during chondrule formation. *Geochim. Cosmochim. Acta* **59**, 2095–2104.

Yurimoto H. and Kuramoto K. (2004) Molecular cloud origin for the oxygen isotope heterogeneity in the solar system. *Science* **305**, 1763–1766.

Yurimoto H., Kuramoto K., Krot A. N., Scott E. R. D., Cuzzi J. N., Thiemens M. H. and Lyons J. R. (2007) Origin and evolution of oxygen isotopic compositions of the solar system. In *Protostars and Planets V* (eds. B. Reipurth, D. Jewitt and K. Keil). University of Arizona Press, Tucson, pp. 849–862.

Ziegler J. F., Biersack J. P. and Littmark U. (1985). In *The Stopping and Ranges of Ions in Matter*, vol. 1. Pergamon, New York, 321 pp.

Associate editor: Alexander N. Krot